

1  
2  
3  
4  
5  
6  
7  
8  
9  
10  
11  
12  
13  
14  
15  
16  
17  
18  
19  
20  
21  
22  
23  
24  
25  
26  
27  
28  
29  
30  
31  
32  
33  
34  
35  
36  
37  
38  
39  
40  
41  
42  
43  
44  
45  
46  
47  
48  
49  
50  
51  
52  
53  
54  
55  
56  
57  
58  
59  
60

# The polymethoxyflavone Sudachitin modulates the circadian clock and improves liver physiology

Kazuaki Mawatari<sup>1,2\*</sup>, Nobuya Koike<sup>3</sup>, Kazuanri Nohara<sup>1</sup>, Marvin Wirianto<sup>1</sup>, Takashi Uebanso<sup>2</sup>, Takaaki Shimohata<sup>2</sup>, Yasuhiro Shikishima<sup>4</sup>, Hiroyuki Miura<sup>4</sup>, Yoshitaka Nii<sup>5</sup>, Mark J. Burish<sup>1</sup>, Kazuhiro Yagita<sup>3</sup>, Akira Takahashi<sup>2</sup>, Seung-Hee Yoo<sup>1</sup>, Zheng Chen<sup>1\*</sup>.

<sup>1</sup>Department of Biochemistry and Molecular Biology, The University of Texas Health Science Center at Houston, 6431 Fannin St., Houston, Texas 77030, U.S.A.

<sup>2</sup>Department of Preventive Environment and Nutrition, Institute of Biomedical Sciences, Tokushima University Graduate School, Kuramoto-cho 3-18-15, Tokushima City, Tokushima 770-8503, Japan.

<sup>3</sup>Department of Physiology and Systems Bioscience, Kyoto Prefectural University of Medicine, Kyoto, 602-8566, Japan

1  
2  
3  
4  
5  
6  
7  
8  
9  
10  
11  
12  
13  
14  
15  
16  
17  
18  
19  
20  
21  
22  
23  
24  
25  
26  
27  
28  
29  
30  
31  
32  
33  
34  
35  
36  
37  
38  
39  
40  
41  
42  
43  
44  
45  
46  
47  
48  
49  
50  
51  
52  
53  
54  
55  
56  
57  
58  
59  
60

<sup>4</sup>Ikeda Yakusou Corporation, 1808-1 Shuzunakatsu, Ikeda-cho, Miyoshi-city, Tokushima 778-0020

<sup>5</sup>Food and Biotechnology Division, Tokushima Prefectural Industrial Technology Center, 11-2 Saika-cho, Tokushima 770-8021, Japan

\*Corresponding authors: [Zheng.Chen.1@uth.tmc.edu](mailto:Zheng.Chen.1@uth.tmc.edu) (Zheng Chen) and [mawatari@tokushima-u.ac.jp](mailto:mawatari@tokushima-u.ac.jp) (Kazuaki Mawatari)

### Keywords

Circadian rhythms, hepatic physiology, multi-omics, polymethoxyflavone, sudachitin.

**ABSTRACT**

Scope: Polymethoxylated flavones (PMFs) are a group of natural compounds known to display a wide array of beneficial effects to promote physiological fitness. Recent studies revealed circadian clocks as an important cellular mechanism mediating preventive efficacy of the major PMF Nobiletin against metabolic disorders. Sudachitin is a PMF enriched in *Citrus sudachi*, and its functions and mechanism of action are poorly understood.

Methods and Results: Using circadian reporter cells, we showed that Sudachitin modulated circadian amplitude and period of *Bmal1* promoter-driven reporter rhythms, and real-time qPCR analysis showed that Sudachitin altered expression of core clock genes, notably *Bmal1*, at both transcript and protein levels. Mass-spec analysis revealed systemic exposure *in vivo*. In mice fed with high-fat diet with or without Sudachitin, we observed increased nighttime activity and daytime sleep, accompanied by significant metabolic improvements in a circadian time-dependent manner, including respiratory quotient, blood lipid and glucose profiles and liver physiology. Focusing on liver, RNA-sequencing and metabolomic analyses revealed prevalent diurnal alteration in both gene expression and metabolite accumulation.

Conclusion: Our study elucidates Sudachitin as a new clock-modulating PMF with beneficial effects to improve diurnal metabolic homeostasis and liver physiology, suggesting the circadian clock as a fundamental mechanism to safeguard physiological well-being.

## 1. Introduction

Natural flavonoids are ubiquitously present in plants and known to display a wide spectrum of biological activities. Of particular interest are polymethoxylated flavones (PMFs) that have shown favorable pharmacokinetic profiles and robust efficacies [1-3]. PMFs are primarily enriched in citrus peels, and various components or extracts have demonstrated anti-inflammatory, metabolic, chemopreventive and neuroprotective activities in cell culture, rodent models and human studies. Nobiletin (NOB, hexa-methoxylated) and Tangeretin (penta-methoxylated) are two well-studied PMFs [1, 3-5]. Compared with hydroxylated analogs lacking the methoxyl groups, these PMFs are more lipophilic and display greater bioavailability due to enhanced transport and metabolic stability, contributing to a superior bioactivity [2]. For example, NOB has been found to effectively improve cholesterol/lipid metabolism in atherosclerogenic *Ldlr*<sup>-/-</sup> mice when incorporated in the diet at 0.1% (w/w) [6], whereas Naringenin, its analog lacking methoxyl groups, was used in similar mouse experiments at 1% (w/w) or higher [7, 8]. Sudachitin is a PMF enriched in the peels of *Citrus sudachi* widely grown in Tokushima, Japan, and has been found to promote energy metabolism and skeletal muscle mitochondria in mice [9-11]. However, unlike other better-known PMFs, biological activities of Sudachitin, especially *in vivo*, remain poorly characterized.

Given the excellent bioactivity and safety characteristics of PMFs as nutritional supplements and potential intervention molecules, it is important to delineate their mechanisms of action in disease models. Recent studies suggest the circadian clock as a possible cellular mechanism underlying efficacies of certain PMFs, notably NOB [12]. The circadian clock is an internal

1  
2  
3 timing device that governs the daily life of cells and organisms [13]. In mammals,  
4  
5  
6 synchronized by the master pacemaker in the hypothalamus, cells throughout the body harbor  
7  
8 a ubiquitous cellular oscillator consisting of positive and negative components forming  
9  
10 negative feedback loops [14-16]. These cell-autonomous oscillators orchestrate cell- and  
11  
12 tissue-specific gene expression programs, supporting specific physiological functions at  
13  
14 individual organs [17-19]. Extensive previous research has revealed that one of the most  
15  
16 fundamental functions of the circadian clock is metabolic regulation [20-22]. Metabolic gene  
17  
18 expression, activities of enzymes/nutrient sensors/transporters, and metabolites have all been  
19  
20 shown to undergo robust circadian oscillation in various tissues, cells and organelles [18, 23].  
21  
22 On the other hand, such metabolic rhythms were largely abolished in genetic models where  
23  
24 circadian rhythms were disrupted or severely dampened due to core clock gene deficiency. In  
25  
26 these circadian mutant mice, a number of metabolic disorders have been demonstrated; for  
27  
28 example, the *Clock $\Delta$ 19* mutant mice were found to be obesity-prone when fed with high-fat  
29  
30 diet or at older ages [24]. The correlation of circadian dysregulation and metabolic disease is  
31  
32 of particular interest because modernization of human societies has led to prevalent circadian  
33  
34 disruptions including shiftwork, light pollution and other facets of 24/7 lifestyles, which  
35  
36 coincides with the escalating epidemic of the metabolic syndrome (e.g., obesity and insulin  
37  
38 resistance).  
39  
40  
41  
42  
43  
44

45  
46 Recently we reported a circadian regulatory function in the physiological efficacy of NOB [12].  
47  
48 In a high-throughput screen to identify clock-targeting molecules, NOB and its close analog  
49  
50 Tangeretin were found to enhance circadian amplitude in reporter cells [25]. More detailed  
51  
52 analyses focusing on NOB showed that NOB directly targets circadian oscillators, which  
53  
54 markedly improves systemic energy homeostasis in diet-induced obese mice and diabetic mice.  
55  
56

1  
2  
3 Through transcriptomics/metabolomics coupled with functional assays, NOB was found to  
4 exert systemic effects to reshape circadian gene oscillations in both liver and skeletal muscle  
5 tissues [25, 26], promoting metabolic health in young and aged mice. The link between  
6 circadian and metabolic functions of NOB has also been demonstrated in other organ systems  
7 and pathophysiological conditions [12, 27-31]. Together, these studies support the notion that  
8 the systemic effects of NOB, and perhaps other PMFs, are in part mediated by the circadian  
9 clock system.  
10  
11  
12  
13  
14  
15  
16  
17  
18  
19  
20

21 In the current study, we investigated whether Sudachitin is a novel clock-modulating PMF that  
22 functions to promote metabolic health. Using circadian reporter cell lines, we found that  
23 Sudachitin strongly activated the circadian amplitude of *Bmall* promoter-directed reporter  
24 expression *in vitro*, and modulated core clock gene expression, particularly *Bmall*, as revealed  
25 by qPCR and immunoblotting. Mass-spec analysis revealed systemic exposure. In mice fed  
26 with high-fat diet with or without Sudachitin, we observed enhanced wheel-running activity,  
27 lengthened free-running periods, and elevated daytime sleep, accompanied by significant  
28 metabolic improvements in both systemic and liver metabolism. Focusing on liver, RNA-  
29 sequencing and metabolomic analyses revealed diurnal circadian and metabolic alterations in  
30 response to Sudachitin. Therefore, these results elucidate Sudachitin as a new clock-  
31 modulating PMF with strong systemic and hepatic efficacies to improve metabolic  
32 homeostasis. These studies also highlight the circadian clock as a fundamental mechanism to  
33 safeguard physiological wellbeing.  
34  
35  
36  
37  
38  
39  
40  
41  
42  
43  
44  
45  
46  
47  
48  
49  
50  
51  
52  
53  
54

## 55 2. Materials and methods

56  
57  
58  
59  
60

## 2.1. Cell culture studies

*Bmal1-luc*-expressing U2OS cells expressing *Bmal1-dGluc* [32] and *Per2::LucSV* mouse fibroblast cells established from adult *Per2::LucSV* knock-in mice [33, 34] were used for real-time bioluminescence monitoring. Cells were grown to confluency on 35 mm dishes in DMEM supplemented with 10% fetal bovine serum, 100 unit/mL penicillin, and 100 µg/mL streptomycin (GenDepot, Katy, TX, USA). Cells were synchronized with 200 nM dexamethasone (Sigma–Aldrich, St. Louis, MO, USA) for 1 hr, and then the media were replaced by luciferin-containing recording media [33, 34] supplemented with vehicle (dimethyl sulfoxide, DMSO) or 1–10 µM Sudachitin (Fujifilm WAKO chemicals, Osaka, Japan). The dishes were tightly sealed with vacuum grease and placed in a luminometer (LumiCycle 32, Actimetrics, Wilmette, IL, USA) for continuous bioluminescence monitoring over 5-7 days. The data were detrended and fitted to a sine wave for measurement of circadian parameters in the LumiCycle data analysis software (Actimetrics). For measurements of mRNA and protein levels of core clock genes, cells were synchronized with 200 nM dexamethasone for 1 hr, and incubated in fresh media containing vehicle (DMSO) or 10 µM Sudachitin. Cells were harvested every 4 hrs for 28 hrs for total RNA and protein extraction.

## 2.2. Purification of Sudachitin for animal treatment

The green peels of *Citrus sudachi* Hort. ex Shirai were collected in Tokushima Prefecture, Japan. The dried peel extracts with 40% ethanol were dissolved with water and fractioned using a synthetic adsorbent DIAION™ HP20 (Mitsubishi Chemical, Tokyo, Japan). The fractions eluted with 30-50% ethanol were dried-up, hydrolyzed by hydrochloric acid, and mixed with ethyl acetate. The hydrophobic fractions were dried and dissolved with 80% ethanol, and fractionated by using the Sephadex® LH-20 column (Cytiva, Tokyo, Japan). The highly concentrated fraction was dried and crystallized under room temperature. The purity of the purified Sudachitin was measured by using the Agilent 1260 Infinity LC system (Agilent Technologies, Santa Clara, CA, USA).

## 2.3. Animal Studies

A schematic diagram to indicate the timeline for animal studies is shown in Fig. S1. Four-week-old male C57BL/6J mice were purchased from the Jackson Laboratory (Bar Harbor, ME, USA). After four weeks of acclimation, the mice were fed with 45 cal% high-fat diet (HFD) (Research Diets, New Brunswick, NJ, USA) *ad libitum* and treated with either vehicle (PBS, n = 11) or Sudachitin (100 mg/kg body weight, n = 12) *via* oral gavage during ZT8-10 every other day. Note that ZT refers to zeitgeber time, with ZT0 and ZT12 corresponding to light on and off respectively. Body weight and food intake were monitored weekly. Tissue samples were collected from 30-week-old mice at the indicated circadian times (ZT6 and ZT18). All animal studies were approved by the Center for Laboratory Animal Medicine and Care

1  
2  
3 (CLAMC) in the University of Texas Health Science Center at Houston, protocol number:  
4  
5 AWC-17-0043, and were conducted in compliance with CLAMC-designated guidelines. The  
6  
7 mouse facility is specific-pathogen free and is tested with sentinel mice monthly.  
8  
9

#### 10 11 12 **2.4. Dosage regimen of Sudachitin for mice**

13  
14  
15 The HFD-fed mice were treated with either vehicle or Sudachitin (100 mg/kg body weight) *via*  
16  
17 oral gavage in late afternoon (ZT8-10) every other day throughout the experimental period and  
18  
19 the behavior analyses. There are two main reasons why we chose this dosing scheme. First, in  
20  
21 our previous study [25] where we investigated the efficacy of another natural clock-  
22  
23 modulating compound, NOB, we used a similar dosing design (oral gavage every other day)  
24  
25 which revealed significant efficacies. The half-life of Nobiletin, at least in the plasma, was  
26  
27 similar to of Sudachitin (1.8 hr vs. 1.7 hr) [35]. Second, given the limited amount of the  
28  
29 compound which is not commercially available in large quantities, this dosing frequency was  
30  
31 designed to optimize exposure throughout the entire study.  
32  
33  
34  
35  
36  
37

#### 38 **2.5. Pharmacokinetic studies in mice**

39  
40 Sudachitin was administered orally at ZT2 at 100 mg/kg in PBS suspension. Eight-week-old  
41  
42 **wild-type** male mice (n = 4 per time point) were sacrificed at 0, 1, 2, 4, 8 and 24 hrs after oral  
43  
44 gavage. Sudachitin and the derivatives in plasma, brain, liver, white adipose tissue (epididymal  
45  
46 fat), brown adipose tissue, and skeletal (soleus) muscle were determined by LC-TOFMS  
47  
48 (Agilent Technologies), as described in Section. 2.15. **Similarly, Sudachitin was administered**  
49  
50  
51  
52  
53  
54  
55  
56  
57  
58  
59  
60

1  
2  
3 at ZT2 to mice either fed under normal conditions or overnight fasted and its brain  
4  
5 accumulation was measured at 0.5 and 1.0 hr after oral gavage.  
6  
7  
8  
9

### 10 **2.6. Mouse wheel-running behavior**

11  
12 Twenty-four-week-old mice were acclimated in individual cages equipped with running  
13 wheels for 3 weeks under the normal 12 hr light/12 hr dark (LD) cycle, followed by 3 weeks in  
14 constant darkness (DD). Activity data were recorded continuously and analyzed using the  
15 CLOCKLAB software (Actimetrics). Free-running periods were calculated using a  
16 periodogram with 6 min resolution. Wheel-running activity levels under both LD and DD  
17 conditions were quantified as a summation every 20 min for each mouse and averaged during  
18 the 2-week data collection.  
19  
20  
21  
22  
23  
24  
25  
26  
27  
28  
29  
30

### 31 **2.7. Noninvasive piezoelectric transducer sleep/wake recording**

32  
33 Sleep/wake recording was carried out by using a noninvasive piezoelectric transducer  
34 sleep/wake recording system (Signal Solutions, Lexington, KY, USA) as previously described  
35 [36]. Briefly, mice were single-housed in the Piezo system with free access to food and water  
36 under the normal LD cycles. The initial 48 hr acclimation period was followed by data  
37 recording for 2 days.  
38  
39  
40  
41  
42  
43  
44  
45  
46

### 47 **2.8. Measurement of energy expenditure**

48  
49 Energy expenditure was examined by measuring oxygen consumption with indirect  
50 calorimetry as previously described [25, 26]. Sixteen-week-old mice were placed at room  
51 temperature (22°C–24°C) in Comprehensive Lab Animal Monitoring System (CLAMS,  
52  
53  
54  
55  
56

1  
2  
3 Columbus Instruments, Columbus, OH, USA) metabolic chambers. Volume of O<sub>2</sub>  
4 consumption (VO<sub>2</sub>) and CO<sub>2</sub> production (VCO<sub>2</sub>) was continuously recorded over a 24-hr  
5  
6  
7 period. Energy expenditure was calculated by average O<sub>2</sub> consumption. Respiratory exchange  
8  
9  
10 ratio (RER) was calculated as the VCO<sub>2</sub>/ VO<sub>2</sub> ratio.  
11  
12  
13

### 14 15 **2.9. Glucose tolerance test**

16  
17 Glucose tolerance test was conducted as previously reported [25, 26]. After overnight fasting,  
18  
19  
20 twenty-week-old mice were weighed prior to glucose injection (1 mg/kg body weight) at ZT2.  
21  
22 Blood glucose was measured at 0, 15, 30, 60, and 120 min after glucose challenge.  
23  
24  
25

### 26 27 **2.10. Plasma Content Assays**

28  
29 Plasma samples were collected from tail vein of twenty-week-old mice after overnight fasting  
30  
31  
32 or without fasting. Plasma insulin was measured by ELISA (Morinaga Institute of Biological  
33  
34  
35 Science, Yokohama, Japan). Plasma triglyceride (TG), total cholesterol, and non-esterified  
36  
37  
38 fatty acid (NEFA) were measured by colorimetric assays (Fujifilm Wako chemicals). Plasma  
39  
40  
41 alanine transaminase (ALT) was measured by a colorimetric assay (Cayman chemicals, Ann  
42  
43  
44 Arbor, MI, USA).  
45

### 46 47 **2.11. RNA extraction and real-time RT-qPCR analysis**

48  
49 RNA extraction and RT-qPCR analysis were carried out as previously described [25, 26].  
50  
51  
52 Total RNA from *Bmall-luc* U2OS cells and mouse liver was isolated using PureXtract  
53  
54  
55  
56  
57  
58  
59  
60

1  
2  
3  
4 RNAsol® reagent (GenDEPOT). RT reactions were performed with 200 ng purified RNAs.

5  
6  
7 *Gapdh* and *act-b* were used as controls. The primer sets used are shown in Table S1.

### 8 9 10 11 **2.12. Western blotting**

12  
13  
14 Western blotting using 15 µg of total protein lysates was performed as previously described  
15  
16  
17 [25, 26]. The following specific antibodies were used, including anti-REV-ERBα (Cell  
18  
19 Signaling Technology, Danvers, MA, USA), anti-PER2 (Sigma–Aldrich), and home-made  
20  
21  
22 antibodies against the other clock proteins [25, 26].  
23  
24  
25  
26

### 27 28 **2.13. Histological analysis**

29  
30 Mouse liver tissues were fixed in 10% neutral buffered formalin and embedded in paraffin.  
31  
32 Sections at 5-µm thickness were stained with hematoxylin–eosin. Histological features were  
33  
34 scored according to the nonalcoholic fatty liver disease (NAFLD) activity scores [37].  
35  
36  
37  
38

### 39 40 **2.14. RNA-sequencing**

41  
42 Two micrograms of extracted RNA from liver (RNA Integrity Number > 9.0, measured by an  
43  
44 Agilent 2100 Bioanalyzer) was used for library construction and RNA sequencing analysis.  
45  
46 PolyA enriched non-stranded RNA sequencing was carried out by Novogene (Sacramento, CA,  
47  
48 USA) on Illumina NovaSeq 6000 with 150-bp paired-end reads, as previously reported [38].  
49  
50 From all sequences, sequence adaptors were removed using Trimmomatic version 0.39 [39].  
51  
52 The sequence reads were mapped to the mouse genome (GRCm38/mm10) using STAR  
53  
54 version 2.7.2a [40]. To obtain reliable alignments, the reads with a mapping quality of less  
55  
56  
57  
58  
59  
60

1  
2  
3 than 10 were removed by SAM tools version 1.7 [41]. The University of California, Santa  
4 Cruz (UCSC) known canonical gene set (55,421) was used for annotation, and the reads  
5 mapped to the exons were quantified using the analyzeRNA.pl script in the Homer software  
6 with an option of `-rpkm` or `-noadj` for FPKM or raw read counts, respectively. Since the  
7 Homer treat each half of the read separately and count each as 0.5 reads for paired-end reads,  
8 the raw read counts were rounded to the nearest integer before analyzing differential expressed  
9 genes using DESeq2 [42]. For gene level analysis, the highest expressed isoform was chosen  
10 to report one isoform per locus. We assumed that a gene was expressed if there were more than  
11  
12 20 reads mapped on average in the exon of the gene. per million reads mapped on average in  
13 the exon of the gene. The expression level cutoff, average FPKM > 0.5, was used for  
14 downstream data analysis. Differentially expressed genes, with threshold of  $p < 0.05$  and fold  
15 change of 1.5, were determined by using DESeq2 [43]. Functional enrichment analysis was  
16 carried out by using Metascape [44].  
17  
18  
19  
20  
21  
22  
23  
24  
25  
26  
27  
28  
29  
30  
31  
32  
33  
34  
35  
36  
37  
38  
39

### 40 **2.15. Metabolomic analysis**

41  
42 The hydrophilic and lipophilic metabolites of liver homogenates were isolated using the Bligh  
43 and Dyer method [45] and measured by CE- and LC-TOFMS, respectively, as previously  
44 described [46]. The  $m/z$  values, retention times or migration time, and ion counts of  
45  
46  
47  
48  
49  
50  
51  
52  
53  
54  
55  
56  
57  
58  
59  
60

1  
2  
3  
4 Extraction method of MassHunter software (Agilent Technologies). The metabolites that  
5  
6  
7 significantly differed between ZT6 and ZT18 in the control and Sudachitin groups ( $P < 0.05$   
8  
9  
10 by one-way analysis of variance) were selected by a multivariate analysis using Mass Profiler  
11  
12  
13 Professional software (Agilent Technologies). The selected metabolites were identified by  
14  
15  
16 using the METLIN Personal Metabolite Database (Agilent Technologies) and LIPID MAPS®  
17  
18  
19 (Wellcome Trust, London, GB). Enrichment analysis of KEGG pathway was carried out by  
20  
21  
22 using MetaboAnalyst 5.0 software [47].  
23  
24  
25  
26  
27  
28

### 29 **2.16. Statistical analysis**

30  
31  
32  
33 Using the CircaCompare rhythmicity software [48, 49], three rhythmic parameters of  
34  
35  
36 endogenous clock genes expression were determined: mesor (mean level), amplitude (half the  
37  
38  
39 range of oscillation), and peak time. Statistical analysis of differences was performed using  
40  
41  
42 ANOVA with Bonferroni's multiple comparison tests using Statview 5.0 software (SAS  
43  
44  
45 Institute Inc., Cary, NC, USA). Student's  $t$ -test was used for paired data where appropriate.  $P <$   
46  
47  
48  
49  
50 0.05 was considered statistically significant.  
51  
52  
53  
54  
55  
56  
57  
58  
59  
60

### 3. Results

#### 3.1. Sudachitin is a clock-modulating compound in cells

To investigate whether Sudachitin functions to modulate circadian clocks, we first tested its efficacy *in vitro*. Two circadian reporter cells were used, including *Bmal1-luc* U2OS cells [32] and *Per2::LucSV* fibroblast cells [33, 34]. The former expresses luciferase transcripts from the *Bmal1* promoter whereas in the latter, the PER2:LUC fusion proteins are driven by the endogenous *Per2* promoter. Interestingly, whereas Sudachitin showed moderate effects in *Per2::LucSV* cells (supplementary Fig. S2), it strongly enhanced the circadian amplitude of the luciferase reporter directed by the *Bmal1* promoter in U2OS cells in a dose-dependent manner (Fig. 1A). In comparison, a period-lengthening effect was detected at 10  $\mu$ M, but not at lower doses (Fig. 1A).

We therefore conducted further molecular analyses using *Bmal1-luc* U2OS cells treated with 10  $\mu$ M Sudachitin to determine core clock gene expression. As shown in Fig. 1B, real-time qPCR analysis revealed that *Bmal1* transcript level was elevated by Sudachitin. The rhythmic parameters, mesor and peak time, of *Bmal1* and *Per2* transcript expression were increased by Sudachitin treatment (supplementary Table S2). In comparison, Sudachitin showed distinct effects on other core clock genes.

Consistent with reporter and qPCR results, BMAL1 protein accumulated to higher levels throughout the circadian cycle and the rhythmic parameters were increased by Sudachitin (Fig. 1C, Table S2). While REV-ERB protein levels were reduced at CT18 and 22, PER2 and CRY1 protein

1  
2  
3 levels were increased by Sudachitin (Fig. 1C). Taken together, Sudachitin shows strong effects on  
4  
5 *Bmal1* expression at both transcript and protein levels, and differentially affects other core clock  
6  
7 components.  
8  
9

### 10 11 12 13 14 15 **3.2 Pharmacokinetics of Sudachitin**

16  
17  
18 To determine the concentrations of Sudachitin and its derivatives in mouse plasma and tissues, we  
19  
20 collected plasma, brain, liver, epididymal fat, brown adipose tissue, and soleus muscle from mice  
21  
22 after oral administration (100 mg/kg body weight) and performed LC-TOFMS. The Sudachitin  
23  
24 compound used was originally purified from *Citrus sudachi* and consisted of approximately 85%  
25  
26 Sudachitin and 15% Demethoxysudachitin (Fig. 2A). Concentrations of Sudachitin in the plasma  
27  
28 and all tissues were significantly increased at 1 hr after oral administration and higher than the  
29  
30 glucuronide derivative and Demethoxysudachitin (Fig. 2C), suggesting a predominantly aglycon  
31  
32 form in mouse tissues. In addition, it accumulated in the liver to a much higher level than in other  
33  
34 tissues (Fig. 2B), suggesting that the liver is a key target tissue.  
35  
36  
37  
38  
39  
40  
41  
42

### 43 **3.3 Sudachitin modulates mouse wheel-running behavior and energy metabolism**

44  
45  
46 Previously we showed that NOB was able to counteract metabolic challenge by high-fat diet to  
47  
48 improve energy homeostasis in mice [25]. We therefore treated HFD-fed wild-type C57BL/6J  
49  
50 mice with Sudachitin *via oral gavage during the inactive phase as previously performed* [25]  
51  
52 *(supplementary Fig. S3A)* and investigated its effects on circadian behavior and energy  
53  
54  
55  
56

1  
2  
3 metabolism. Sudachitin treatment was able to increase wheel-running activity in the middle of  
4  
5  
6 nighttime (Fig. 3A-B) and interestingly also lengthened the free-running period under DD  
7  
8 conditions (Fig. 3C). In the non-invasive Piezo sleep recording experiment, we found that  
9  
10 Sudachitin increased daytime and total sleep amounts (Fig. 3D). Together, these results reveal *in*  
11  
12 *vivo* efficacies of Sudachitin in clock-directed activity and sleep behaviors.  
13  
14

15  
16 We next examined energy metabolism in these mice. Sudachitin treatment did not lead to  
17  
18 significant changes in body weight or food intake (supplementary Fig. S3B-C). In metabolic  
19  
20 chambers, sudachitin-treated mice show reduced respiratory exchange rates (RER) (Fig. 3F),  
21  
22 suggesting upregulation of lipid utilization, whereas oxygen consumption was not significantly  
23  
24 altered (Fig. 3E). We next examined circulating lipid and glucose profiles. Plasma triglyceride and  
25  
26 NEFA levels were significantly reduced by Sudachitin under the fed, but not fasted, condition (Fig.  
27  
28 4, A-B), and plasma cholesterol levels remained unchanged (Fig. 4C). Likewise, blood glucose  
29  
30 and insulin levels were reduced by Sudachitin only in the fed condition (Fig. 4, D-E). Glucose  
31  
32 tolerance test revealed a trend of improvement in Sudachitin-treated mice relative to control mice  
33  
34 (supplementary Fig. S3D-E).  
35  
36  
37  
38

39  
40 Consistent with largely constant body weight, weights of individual tissues, including liver,  
41  
42 epididymal and subcutaneous fat, brown fat and skeletal muscle, were not altered by Sudachitin  
43  
44 (supplementary Fig. S3F). On the other hand, H&E staining of the liver showed that both steatosis  
45  
46 and hepatocellular ballooning [37] were reduced by Sudachitin (Fig. 4F). In accordance, the  
47  
48 NAFLD activity score showed a trend of reduction in response to Sudachitin, and liver triglyceride  
49  
50 content was reduced in Sudachitin-treated mice at ZT18 (Fig. 4, G-H). On the other hand, NEFA  
51  
52 and cholesterol levels in the liver were not changed (supplementary Fig. S3G-H). As a marker of  
53  
54  
55  
56  
57  
58  
59  
60

1  
2  
3 liver damage, plasma ALT activity was alleviated by Sudachitin (Fig. 4I). Additionally, mRNA  
4 levels of the genes involved in fibrosis (*Timp1*, *Tgfb1*) and inflammation (*Mcp1*, *Tnfa*) were  
5 lowered at ZT18 by Sudachitin (Fig. 4J). Together, these results support a beneficial role of  
6 Sudachitin to improve energy metabolism in HFD-fed WT mice.  
7  
8  
9  
10  
11

### 12 13 14 15 16 17 **3.4 Transcriptomic alteration in the liver by Sudachitin**

18  
19  
20 Given the observed beneficial effects of Sudachitin in the liver, we focused on this central  
21 metabolic organ and applied omics approaches to globally survey Sudachitin-induced molecular  
22 alteration. First we conducted transcriptomics by RNA-sequencing using RNA samples from  
23 livers isolated from control and sudachitin treated mice at ZT6 and ZT18 (daytime and nighttime,  
24 respectively) (NCBI GEO accession number: GSE211612). Gene expression comparison between  
25 the two time points revealed 632 and 651 diurnal DEGs (differential expressed genes) in the  
26 control and Sudachitin groups respectively ( $p < 0.05$ , fold change  $>1.5$ ) (Fig. 5, A-B, Table S3);  
27 among them, 243 genes were shared between the groups, suggesting an intrinsic, Sudachitin-  
28 independent oscillatory pattern (Fig. 5B). Metascape analysis [44] revealed enrichment of  
29 functional pathways, including lipid/fatty acid metabolism in the control group, PPAR signaling,  
30 circadian rhythm, and lipid catabolism in the sudachitin group, and acylglycerol metabolism  
31 shared between the groups (Fig. 5C). These results highlight a modulatory role of Sudachitin in  
32 hepatic circadian and lipid metabolic pathways.  
33  
34  
35  
36  
37  
38  
39  
40  
41  
42  
43  
44  
45  
46  
47  
48  
49  
50

51 To validate the profiling results, we examined mRNA levels of selected circadian and lipid  
52 metabolic genes by real-time qPCR (Fig. 5D-F). We found diurnal expression of core clock genes  
53  
54  
55  
56

1  
2  
3 in both groups including *Per2*, *Rev-erba*, *Cry1*, and *Rorc* (Fig. 5D). In comparison, *Per1* showed  
4 altered phase in response to Sudachitin, and the levels of *Per1* and *Per2* at ZT6 and *Rev-erba* at  
5 ZT18 were statistically different between the two groups (Fig. 5D). Furthermore, several genes  
6 involved in lipid metabolism including *Insig1*, *Srebf2*, *Hmgcs2*, *Elvol6*, and *Acot3* displayed  
7 diurnal expression in both groups (supplementary Fig. S4). Group-specific diurnal expressions  
8 were also observed, including *Cyp7a1*, *Ppard*, *Ppara*, and *Acot3* in the control group (Fig. 5E) and  
9 *Fasn*, *Fads*, and *Acly* in the sudachitin group (Fig. 5F). In addition, the levels of *Cyp7a1*, *Acly*, and  
10 *Acaca* at ZT6 and *Ppard* at ZT18 were statistically different between the two groups (Figs. 5E-F,  
11 S4). These results together indicate transcriptomic modulation in the liver by Sudachitin, notably  
12 in circadian and lipid metabolic pathways.  
13  
14  
15  
16  
17  
18  
19  
20  
21  
22  
23  
24  
25  
26  
27  
28  
29  
30

### 31 **3.5. Metabolomic alteration in the liver by Sudachitin**

32  
33  
34 To investigate how Sudachitin alters the metabolomic landscape in the liver, we prepared both  
35 hydrophilic and lipophilic fractions from the liver. First, the hydrophilic fractions were subjected  
36 to CE-TOFMS analysis and 90 metabolites were identified by a standard metabolites reference kit  
37 (HMT, Tsuruoka, Japan). Between the two time points 31 and 14 metabolites showed diurnal  
38 alteration in the control and Sudachitin groups respectively ( $p < 0.05$ ) (Fig. 6A-B, Table S4),  
39 including 5 metabolites shared between the groups (Fig. 6B). PCA analysis revealed significant  
40 changes at ZT6 in response to Sudachitin (Fig. 6C). Enrichment analysis by MetaboAnalyst 5.0  
41 software [47] showed greater enrichment of citrate cycle, pyruvate metabolism, and amino acid  
42 metabolism pathways in the control group compared with the Sudachitin group (Fig. 6D, S5A-B).  
43  
44  
45  
46  
47  
48  
49  
50  
51  
52  
53  
54  
55  
56  
57  
58  
59  
60

1  
2  
3 S5C), pyruvate metabolism (Fig. S5C), branched-chain amino acid metabolism (Fig. 6F), aromatic  
4 amino acid metabolism (Fig. 6G), and cysteine and methionine metabolism (Fig. S5D) showed  
5 diurnal changes in the control group, and at significantly lower concentrations ( $p < 0.05$ , in  
6 mmol/g tissue) than in the Sudachitin group at ZT6. These results highlight a modulatory role of  
7 Sudachitin in hepatic glucose and amino acid metabolism pathways.  
8  
9

10  
11  
12  
13  
14  
15  
16 Next, LC-TOFMS analysis of the lipophilic fractions identified 706 metabolites, significantly  
17 more than those in the hydrophilic fractions. Between the two time points 75 and 14 metabolites  
18 showed diurnal fluctuation in the control and Sudachitin groups respectively ( $p < 0.05$ ) (Fig. 7, A-  
19 B, Table S5); including 3 metabolites shared between the groups (Fig. 7B). In addition, PCA  
20 analysis revealed significant changes at both ZT6 and ZT18 in response to Sudachitin (Fig. 7C).  
21  
22

23  
24  
25 Cross-referencing the METLIN and LIPID MAPS® databases identified distinct metabolites  
26 between the control and Sudachitin groups including peptides, phosphoglycerolipids, and  
27 sphingolipids. For example, tetra/penta-peptides (Fig. 7E, S6A) and phosphoglycerolipids  
28 including phosphatidylcholine (PC) and phosphatidylinositol (PI) (Fig. 7F, S6B) showed diurnal  
29 changes in the control group and significantly lower levels at ZT18 than in the Sudachitin group.  
30  
31 At ZT6, sphingolipids including sphingosine and sphinganine (Fig. 7F) and other  
32 phosphoglycerolipids (Fig. S6C) showed diurnal changes in the control group and significantly  
33 lower levels than the Sudachitin group. These results highlight a modulatory role of Sudachitin in  
34 hepatic phospholipids and peptide metabolisms.  
35  
36  
37  
38  
39  
40  
41  
42  
43  
44  
45  
46  
47  
48  
49  
50  
51  
52

#### 53 **4. Discussion**

54  
55  
56  
57  
58  
59  
60

1  
2  
3  
4 The circadian clock constitutes a key regulatory mechanism of energy metabolism, and  
5  
6  
7 previous studies demonstrate a clock-targeting efficacy of the major PMF Nobiletin [12]. In  
8  
9  
10 the current study, we explored a potential circadian and metabolic efficacy of Sudachitin, a  
11  
12  
13 natural PMF enriched in the peels of *Citrus sudachi* that is highly abundant in the Tokushima  
14  
15  
16 region. Interestingly, our results reveal novel circadian and metabolic activities of this under-  
17  
18  
19 studied PMF, providing valuable mechanistic and functional insights into this bioactive PMF.  
20  
21  
22  
23  
24 Our *in vitro* and *in vivo* studies provide strong evidence for the clock-altering activities of  
25  
26  
27 Sudachitin. Interestingly, compared with NOB [25], Sudachitin showed moderate effects on  
28  
29  
30 PER2::LUC rhythms; rather, it enhanced *Bmal1* promoter-driven transcription as revealed by  
31  
32  
33 *Bmal1-luc* reporter cells and BMAL1 protein expression analysis. Consistent with these *in*  
34  
35  
36 *vitro* effects, in HFD-fed WT mice, Sudachitin was also found to increase nighttime wheel-  
37  
38  
39 running activity as well as daytime sleep, supporting a role of Sudachitin to potentiate  
40  
41  
42 circadian behavioral rhythms. The molecular mechanism and target of Sudachitin underlying  
43  
44  
45 the clock-modulatory activities remain to be investigated. Previously NOB was found to bind  
46  
47  
48 to and activate ROR receptors, core clock components in the secondary loop known to  
49  
50  
51 promote circadian robustness and stability [25]. However, given the distinct effects of  
52  
53  
54  
55  
56  
57  
58  
59  
60

1  
2  
3  
4 Sudachitin on reporter rhythms and core clock gene expression, it is likely that Sudachitin may  
5  
6  
7 act through a different mechanism in the circadian oscillator. Both qPCR and immunoblotting  
8  
9  
10 results appear to underscore a strong effect of Sudachitin on *Bmall* expression, at both  
11  
12 transcript and protein levels. *Bmall* is tightly controlled by the secondary loop including both  
13  
14 RORs and REV-ERBs [15]. Interestingly, our results show that Sudachitin reduces the  
15  
16 transcript and protein levels of REV-ERBs, providing a possible explanation for the increased  
17  
18 *Bmall* expression. Finally, we adopted a similar alternate-day administration of Sudachitin as  
19  
20 previous described for NOB [25]. The half-life of NOB, at least in the plasma, is similar to that  
21  
22 of Sudachitin **under the acute PK study conditions** (1.8 hr vs. 1.7 hr) [35]. The reason  
23  
24 underlying the circadian and physiological effects despite the relatively short half-life is  
25  
26 unclear, but could involve sustained downstream action after the initial binding of compounds  
27  
28 to their cellular targets and/or activity of their metabolic derivatives as reported previously for  
29  
30 NOB [50, 51]. **Furthermore, while a single dose was administered in the PK study, our *in vivo***  
31  
32 **experiments entailed a chronic treatment regimen. Another variable is the feeding condition.**  
33  
34 **The time of gavage at ZT8-10 for our *in vivo* studies corresponds to a fasting condition, and**  
35  
36 **our PK study (supplementary Fig. S3A) showed that Sudachitin accumulates in the brain at**  
37  
38 **higher levels in fasted mice compared with fed mice.** Follow-up studies should further  
39  
40 characterize *in vivo* effects of Sudachitin in physiological settings over a full circadian time  
41  
42 course **under different feeding and treatment conditions.**

43  
44  
45  
46  
47  
48  
49  
50 Circadian regulation of energy metabolism is well established [17]. In a pioneering study, it  
51  
52 has been shown that circadian disruption exacerbates the metabolic syndrome induced by  
53  
54 nutrient excess in HFD-fed mice [24]. We previously showed that circadian enhancement by  
55  
56

1  
2  
3 NOB was able to counteract the adverse effects of HFD, markedly improving systemic energy  
4 homeostasis and tissue metabolism in liver and skeletal muscle [25, 26]. The metabolic effects  
5 of Sudachitin have not been well characterized. Notably, in one study where Sudachitin was  
6 administered to mice suffering from metabolic syndrome, energy homeostasis was found to be  
7 improved, accompanied by enhanced mitochondrial biogenesis in skeletal muscle [9]. To  
8 further examine the effects of Sudachitin against metabolic challenge, especially in light of its  
9 clock-enhancing activities, we treated WT mice fed with HFD with Sudachitin. While we did  
10 not find changes in body weight, several systemic metabolic parameters were improved,  
11 including reduced respiratory exchange rate and lower lipid levels in circulation. Both findings  
12 suggest diminished lipid utilization under the HFD conditions as a result of Sudachitin  
13 treatment. We also found that plasma glucose and insulin levels were reduced under fed  
14 conditions, consistent with a trend of improved glucose tolerance. While liver, adipose and  
15 muscle tissue weights were largely unchanged in accordance with the body weight pattern,  
16 several aspects of liver physiologies were improved, including lipid accumulation and liver  
17 damage. This is consistent with our previous results that liver is a key target organ for clock  
18 regulation and NOB strongly improve liver health under HFD conditions [25].  
19  
20  
21  
22  
23  
24  
25  
26  
27  
28  
29  
30  
31  
32  
33  
34  
35  
36  
37  
38  
39  
40

41 Liver is the central metabolic organ, orchestrating myriads of metabolic pathways important  
42 for organismal health [52, 53]. We therefore applied powerful omics approaches to survey  
43 hepatic alteration by Sudachitin in a comprehensive and unbiased manner. Transcriptomic  
44 analysis by RNA-seq revealed that Sudachitin modulated diurnal expression of lipid  
45 metabolism-related genes in the liver, including downregulation of *Ppard* known to play a key  
46 role in diurnal regulation of lipogenic gene expression [54]. Patients with nonalcoholic  
47 steatohepatitis (NASH) and NAFLD have been found to display decreased levels of hepatic  
48  
49  
50  
51  
52  
53  
54  
55  
56  
57  
58  
59  
60

1  
2  
3 phospholipids including phosphatidylcholines (PCs) associated with reduced activity of fatty  
4 acid desaturase (FADS) and consequently impaired phospholipids synthesis [55, 56]. In our  
5 study, Sudachitin modulates diurnal patterns of both *fads* gene expression (Fig. 5F) and several  
6 main PCs (Fig. 7F), which may contribute to the improved hepatic steatosis following  
7 Sudachitin treatment. In addition to phospholipids, the Sudachitin group showed higher  
8 hepatic contents of branched-chain amino acids ( BCAAs) at ZT6 than the control group (Fig. 6,  
9 F-G). Enrichment of BCAAs could activate the mTOR pathway, inhibiting fatty acid  
10 conversion to triglycerides and therefore lipid accumulation [57]. BCAAs have also been  
11 shown to ameliorate dysfunction of the mitochondrial TCA cycle in a NASH model [58]. In  
12 accordance, Sudachitin treatment led to higher levels of mitochondrial and the intermediate  
13 metabolites of the TCA cycle at ZT6 compared with the control group (Fig. 6E), analogous to  
14 our previously reported effects of Nobiletin which promotes mitochondrial respiration in  
15 skeletal muscle of aged mice [25, 26].  
16  
17  
18  
19  
20  
21  
22  
23  
24  
25  
26  
27  
28  
29  
30  
31  
32  
33  
34

35 Circadian rhythms are increasingly appreciated as crucially important for health and healthy  
36 aging. Whereas mounting epidemiological and genetic evidence has established a causal role  
37 of circadian disruption in chronic diseases and age-related decline [59-62], how to exploit the  
38 clock as a therapeutic target require further investigations. In addition to chronotherapy that  
39 times the administration of treatment in order to maximize the therapeutic index (efficacy vs  
40 toxicity), a distinct approach is to directly manipulate the intrinsic clocks or clock components  
41 in disease settings [63, 64]. For example, time-restricted feeding, limiting food availability to a  
42  
43  
44  
45  
46  
47  
48  
49  
50  
51  
52  
53  
54  
55  
56  
57  
58  
59  
60

1  
2  
3  
4 restricted time window during the day (~8-10 hrs), has been shown to enhance circadian  
5  
6  
7 metabolic rhythms and show preventive and therapeutic efficacies in preclinical and clinical  
8  
9  
10 studies [65, 66]. A large number of small molecules have also been shown to modulate the  
11  
12  
13 clock and clock-controlled cellular and physiological functions in cells and mouse models [64,  
14  
15  
16 67]. The newly identified clock-modulatory activity of Sudachitin, coupled with its abundant  
17  
18  
19 source and excellent PK and safety profiles, serve as a strong foundation for further research  
20  
21  
22 and development of Sudachitin as a bioactive molecule with promising applications in various  
23  
24  
25  
26  
27 fields ranging from nutrition, disease intervention and healthy aging.  
28  
29  
30  
31  
32  
33  
34  
35  
36

## 37 **Acknowledgements**

38  
39  
40  
41  
42 The excellent technical assistance of Jiah Yang, Randika Parakramaweera, and Jae  
43  
44 Hyung Kim (The University of Texas Health Science Center at Houston) is gratefully  
45  
46 acknowledged. Bmal1-dGluc vector is a generous gift from Dr. Shin Yamazaki. This study  
47  
48 was supported by Support Center for Advanced Medical Sciences, Tokushima University  
49  
50 Graduate School of Biomedical Sciences, and by Support Center for The Special Mission  
51  
52 Center for Metabolome Analysis, School of Medical Nutrition, Faculty of Medicine of  
53  
54  
55  
56

1  
2  
3 Tokushima University, and Support Center for Advanced Medical Sciences, Tokushima  
4  
5 University Graduate School of Biomedical Sciences.  
6  
7  
8  
9  
10  
11  
12

## 13 Author Contributions

14  
15  
16  
17

18 **Kazuaki Mawatari:** Conceptualization, Methodology, Validation, Formal analysis,  
19 Investigation, Writing – original draft, Writing – review & editing, Visualization, Funding  
20 acquisition. **Nobuya Koike:** Methodology, Validation, Formal analysis, Investigation, Writing  
21  
22 – review & editing, Visualization, **Kazunari Nohara:** Methodology, Investigation, Formal  
23 analysis. **Marvin Wirianto:** Methodology, Investigation, Formal analysis. **Takashi Uebanso:**  
24  
25 Methodology, Writing – review & editing. **Takaaki Shimohata:** Methodology. **Yasuhiro**  
26  
27 **Shikishima:** Resources, Methodology. **Hiroyuki Miura:** Resources, Methodology. **Yoshitaka**  
28  
29 **Nii:** Resources, Methodology. **Mark J. Burish:** Resources, Methodology. **Kazuhiro Yagita:**  
30  
31 Methodology, Writing – review & editing. **Akira Takahashi:** Writing – review & editing,  
32  
33 Funding acquisition. **Seung-Hee Yoo:** Supervision, Resources, Methodology, Writing – review  
34  
35  
36  
37  
38  
39  
40  
41  
42  
43  
44  
45  
46  
47  
48  
49  
50  
51  
52  
53  
54  
55  
56  
57  
58  
59  
60

1  
2  
3 & editing, Funding acquisition. **Zheng Chen**: Supervision, Conceptualization, Writing –  
4  
5  
6  
7 review & editing, Project administration, Funding acquisition.  
8  
9

## 16 Declaration of Competing Interest

17  
18  
19  
20  
21  
22 The authors declare no conflict of interest.  
23  
24  
25  
26  
27  
28  
29

## 30 Funding

31  
32  
33  
34  
35 This work was supported by JSPS KAKENHI Grant Numbers 15KK0345 (K.M.) and  
36  
37 18KK0274 (A.T.), and supported by Cabinet Office, Government of Japan, Cross-ministerial  
38  
39 Moonshot Agriculture, Forestry and Fisheries Research and Development Program,  
40  
41 “Technologies for Smart Bio-industry and Agriculture” (funding agency: Bio-oriented  
42  
43 Technology Research Advancement Institution) (JPJ009237). This work is also supported by  
44  
45 the Welch Foundation, Texas, USA (AU-1731-20190330 to Z.C. and AU-1971-20180324 to S.-  
46  
47  
48  
49  
50  
51  
52  
53 H.Y.).  
54  
55  
56  
57  
58  
59  
60

## Data Availability Statement

The RNAseq data were deposited to NCBI GEO (GEO accession number: GSE211612). The DESeq2 results and the metabolomic measurement results with statistical analysis were also listed in the supplementary tables S3-5. The other data that support the findings of this study are available from the corresponding author upon reasonable request.

## References

- [1] T. Walle, *Semin. Cancer Biol.* **2007**, *17*, 354.
- [2] M. Evans, P. Sharma, N. Guthrie, Bioavailability of Citrus Polymethoxylated Flavones and Their Biological Role in Metabolic Syndrome and Hyperlipidemia, IntechOpen, London, United Kingdom **2012**, Ch. 6.
- [3] H. Huang, L. Li, W. Shi, H. Liu, J. Yang, X. Yuan, and L. Wu, *Evid. Based Complement. Alternat. Med.* **2016**, *2016*, 2918796.
- [4] B. Singh, J. P. Singh, A. Kaur, N. Singh, *Food. Res. Int.* **2020**, *132*, 109114.
- [5] E. E. Mulvihill, A. C. Burke, M. W. Huff, *Annu. Rev. Nutr.* **2016**, *36*, 275.
- [6] E. E. Mulvihill, J. M. Assini, J. K. Lee, E. M. Allister, B. G. Sutherland, J. B. Koppes, C. G. Sawyez, J. Y. Edwards, D. E. Telford, A. Charbonneau, P. St-Pierre, A. Marette, M. W. Huff., *Diabetes* **2011**, *60*, 1446.
- [7] E. E. Mulvihill, E. M. Allister, B. G. Sutherland, D. E. Telford, C. G. Sawyez, J. Y. Edwards, J. M. Markle, R. A. Hegele, M. W., *Diabetes* **2009**, *58*, 2198.
- [8] J. M. Assini, E. E. Mulvihill, B. G. Sutherland, D. E. Telford, C. G. Sawyez, S. L. Felder, S. Chhoker, J. Y. Edwards, R. Gros, M. W. Huff, *J. lipid Res.* **2013**, *54*, 711.
- [9] R. Tsutsumi, T. Yoshida, Y. Nii, N. Okahisa, S. Iwata, M. Tsukayama, R. Hashimoto, Y. Taniguchi, H. Sakaue, T. Hosaka, E. Shuto, T. Sakai, *Nutr. Metab. (Lond.)* **2014**, *11*, 32.
- [10] Y. Ohyama, J. Ito, V. J. Kitano, J. Shimada, Y. Hakeda, *PLoS One* **2018**, *13*, e0191192.
- [11] H. Nakagawa, Y. Takaishi, N. Tanaka, K. Tsuchiya, H. Shibata, T. Higuti, *J. Nat. Prod.* **2006**, *69*, 1177.
- [12] E. Mileykovskaya, S. H. Yoo, W. Dowhan, Z. Chen, *Biochemistry* **2020**, *85*, 1554.
- [13] D. Bell-Pedersen, D., V. M. Cassone, D. J. Earnest, S. S. Golden, P. E. Hardin, T. L. Thomas, M. J. Zoran, *Nat. Rev. Genet.* **2005**, *6*, 544.
- [14] J. A. Mohawk, C. B. Green, J. S. Takahashi, *Annu. Rev Neurosci.* **2012**, *35*, 445.
- [15] J. S. Takahashi, *Nat. Rev. Genet.* **2017**, *18*, 164.
- [16] C. L. Partch, *J Mol Biol*, **432**, 3426, 2020.
- [17] J. Bass, M. A. Lazar, *Science* **2016**, *354*, 994.

- 1  
2  
3  
4 [18] R. Zhang, N. F. Lahens, H. I. Ballance, M. E. Hughes, J. B. Hogenesch, *Proc. Natl. Acad. Sci. U. S. A.* **2014**, *111*, 16219.
- 5  
6  
7 [19] L. S. Mure, H. D. Le, G. Benegiamo, M. W. Chang, L. Rios, N. Jillani, M. Ngotho, T. Kariuki, O. Dkhissi-Benyahya, H. M. Cooper, S. Panda, *Science* **2018**, *359*, 6381.
- 8  
9  
10 [20] J. Rutter, M. Reick, S. L. McKnight, *Annu. Rev. Biochem.* **2002**, *71*, 307
- 11  
12 [21] C. B. Green, J. S. Takahashi, J. Bass, *Cell* **2008**, *134*, 728.
- 13  
14 [22] S. Panda, *Science* **2016**, *354*, 1008.
- 15  
16 [23] G. Manella, G. Asher, *Front. Endocrinol.* **2016**, *7*, 162.
- 17  
18 [24] F. W. Turek, C. Joshu, A. Kohsaka, E. Lin, G. Ivanova, E. McDearmon, A. Laposky, S. Losee-Olson, A. Easton, D. R. Jensen, R. H. Eckel, J. S. Takahashi, J. Bass, *Science* **2005**, *308*, 1043.
- 19  
20  
21 [25] B. He, K. Nohara, N. Park, Y. S. Park, B. Guillory, Z. Zhao, J. M. Garcia, N. Koike, C. C. Lee, J. S. Takahashi, S. H. Yoo, Z. Chen, *Cell Metab.* **2016**, *23*, 610.
- 22  
23  
24 [26] K. Nohara, V. Mallampalli, T. Nemkov, M. Wirianto, J. Yang, Y. Ye, Y. Sun, L. Han, K. A. Esser, E. Mileykovskaya, A. D'Alessandro, C. B. Green, J. S. Takahashi, W. Dowhan, S. H. Yoo, Z. Chen, *Nat. Commun.* **2019**, *10*, 3923.
- 25  
26  
27 [27] V. Petrenko, N. R. Gandasi, D. Sage, A. Tengholm, S. Barg, C. Dibner, *Proc. Natl. Acad. Sci. U. S. A.* **2020**, *117*, 2484.
- 28  
29  
30 [28] K. Rakshit, A. V. Matveyenko, *Diabetes* **2021**, *70*, 143.
- 31  
32  
33 [29] K. Nohara, T. Nemkov, A. D'Alessandro, S. H. Yoo, Z. Chen, *Int. J. Mol. Sci.* **2019**, *20*, 4281.
- 34  
35  
36 [30] A. Shinozaki, K. Misawa, Y. Ikeda, A. Haraguchi, M. Kamagata, Y. Tahara, S. Shibata, *PLoS One* **2017**, *12*, e0170904.
- 37  
38  
39 [31] M. Wirianto, C. Y. Wang, E. Kim, N. Koike, R. Gomez-Gutierrez, K. Nohara, G. Escobedo, Jr., J. M. Choi, C. Han, K. Yagita, S. Y. Jung, C. Soto, H. K. Lee, R. Morales, S. H. Yoo, Z. Chen, *FASEB J.* **2022**, *36*, e22186.
- 40  
41  
42 [32] M. Yeom, J. S. Pendergast, Y. Ohmiya, S. Yamazaki, *Proc. Natl. Acad. Sci. U. S. A.* **2010**, *107*, 9665.
- 43  
44  
45 [33] Z. Chen, S. H. Yoo, Y. S. Park, K. H. Kim, S. Wei, E. Buhr, Z. Y. Ye, H. L. Pan, J. S. Takahashi., *Proc. Natl. Acad. Sci. U. S. A.* **2012**, *109*, 101.
- 46  
47  
48 [34] S. H. Yoo, S. Kojima, K. Shimomura, N. Koike, E. D. Buhr, T. Furukawa, C. H. Ko, G. Gloston, C. Ayoub, K. Nohara, B. A. Reyes, Y. Tsuchiya, O. J. Yoo, K. Yagita, C.

- 1  
2  
3  
4 Lee, Z. Chen, S. Yamazaki, C. B. Green, J. S. Takahashi, *Proc. Natl. Acad. Sci. U. S.*  
5 *A.* **2017**, *114*, E8855.  
6  
7 [35] S. P. Singh, D. T. Wahajuddin, K. Patel, G. K. Jain, *Fitoterapia* **2011**, *82*, 1206.  
8  
9 [36] C. Han, M. Wirianto, E. Kim, M. J. Burish, S. H. Yoo, Z. Chen, *Clocks Sleep* **2021**, *3*,  
10 351.  
11  
12 [37] A. C. Sheka, O. Adeyi, J. Thompson, B. Hameed, P. A. Crawford, S. Ikramuddin,  
13 *JAMA* **2020**, *323*, 1175.  
14  
15 [38] H. K. Kim, S. Y. Lee, N. Koike, E. Kim, M. Wirianto, M. J. Burish, K. Yagita, H. K.  
16 Lee, Z. Chen, J. M. Chung, S. Abdi, S. H. Yoo, *Sci. Rep.* **2020**, *10*, 13844.  
17  
18 [39] A. M. Bolger, M. Lohse, and B. Usadel, *Bioinformatics* **2014**, *30*, 2114.  
19  
20 [40] A. Dobin, C. A. Davis, F. Schlesinger, J. Drenkow, C. Zaleski, S. Jha, P. Batut, M.  
21 Chaisson, T. R. Gingeras, *Bioinformatics* **2013**, *29*, 15.  
22  
23 [41] H. Li, B. Handsaker, A. Wysoker, T. Fennell, J. Ruan, N. Homer, G. Marth, G.  
24 Abecasis, R. Durbin, *Bioinformatics* **2009**, *25*, 2078.  
25  
26 [42] S. Heinz, C. Benner, N. Spann, E. Bertolino, Y. C. Lin, P. Laslo, J. X. Cheng, C.  
27 Murre, H. Singh, C. K. Glass, *Mol. Cell* **2010**, *38*, 576.  
28  
29 [43] M. I. Love, W. Huber, S. Anders, *Genome Biol.* **2014**, *15*, 550.  
30  
31 [44] Y. Zhou, B. Zhou, L. Pache, M. Chang, A. H. Khodabakhshi, O. Tanaseichuk, C.  
32 Benner, S. K. Chanda, *Nat. Commun.* **2019**, *10*, 1523.  
33  
34 [45] J. Folch, M. Lees, G. H. Sloane Stanley, *J. Biol. Chem.* **1957**, *226*, 497.  
35  
36 [46] H. Mori, Y. Morine, K. Mawatari, A. Chiba, S. Yamada, Y. U. Saito, H. Ishibashi, A.  
37 Takahashi, M. Shimada, *Anticancer Res.* **2021**, *41*, 327.  
38  
39 [47] Z. Pang, J. Chong, G. Zhou, D. A. de Lima Morais, L. Chang, M. Barrette, C. Gauthier,  
40 P. E. Jacques, S. Li, J. Xia., *Nucleic Acids Res.* **2021**, *49*, W388.  
41  
42 [48] R. Parsons, R. Parsons, N. Garner, H. Oster, O. Rawashdeh, *Bioinformatics* **2020**, *36*,  
43 1208.  
44  
45 [49] S. Deota, H. Calligaro, S. Panda, Design Principles and Analysis Guidelines for  
46 Understanding Time-of-Day Effects in the Brain, Circadian Clocks, Springer Nature,  
47 Switherland **2022**, Ch. 14.  
48  
49 [50] C. DiMarco-Crook, K. Rakariyatham, Z. Li, Z. Du, J. Zheng, X. Wu, H. Xiao, *J Food*  
50 *Sci* **2020**, *85*, 1292.  
51  
52  
53  
54  
55  
56  
57  
58  
59  
60

- 1  
2  
3  
4 [51] M. Al Rahim, A. Nakajima, D. Saigusa, N. Tetsu, Y. Maruyama, M. Shibuya, H.  
5 Yamakoshi, Y. Tomioka, Y. Iwabuchi, Y. Ohizumi, T. Yamakuni, *Biochemistry* **2009**,  
6 *48*, 7713.  
7  
8 [52] S. Panda, M. P. Antoch, B. H. Miller, A. I. Su, A. B. Schook, M. Straume, P. G.  
9 Schultz, S. A. Kay, J. S. Takahashi, J. B. Hogenesch, *Cell* **2002**, *109*, 307.  
10  
11 [53] Y. Adamovich, R. Aviram, G. Asher, *Biochim. Biophys. Acta* **2015**, *1851*, 1017.  
12  
13 [54] S. Liu, J. D. Brown, K. J. Stanya, E. Homan, M. Leidl, K. Inouye, P. Bhargava, M. R.  
14 Gangl, L. Dai, B. Hatano, G. S. Hotamisligil, A. Saghatelian, J. Plutzky, C. H. Lee.,  
15 *Nature* **2013**, *502*, 550.  
16  
17 [55] F. Chiappini, A. Coilly, H. Kadar, P. Gual, A. Tran, C. Desterke, D. Samuel, J. C.  
18 Duclos-Vallee, D. Touboul, J. Bertrand-Michel, A. Brunelle, C. Guettier, F. Le Naour,  
19 *Sci. Rep.* **2017**, *7*, 46658.  
20  
21 [56] K. Y. Peng, M. J. Watt, S. Rensen, J. W. Greve, K. Huynh, K. S. Jayawardana, P. J.  
22 Meikle, R. C. R. Meex, *J. lipid Res.* **2018**, *59*, 1977.  
23  
24 [57] F. Zhang, S. Zhao, W. Yan, Y. Xia, X. Chen, W. Wang, J. Zhang, C. Gao, C. Peng, F.  
25 Yan, H. Zhao, K. Lian, Y. Lee, L. Zhang, W. B. Lau, X. Ma, L. Tao, *EBioMedicine*  
26 **2016**, *3*, 157.  
27  
28 [58] T. Honda, M. Ishigami, F. Luo, M. Lingyun, Y. Ishizu, T. Kuzuya, K. Hayashi, I.  
29 Nakano, T. Ishikawa, G. G. Feng, Y. Katano, T. Kohama, Y. Kitaura, Y. Shimomura,  
30 H. Goto, Y. Hirooka, *Metabolism* **2017**, *69*, 177.  
31  
32 [59] S. Sato, G. Solanas, F. O. Peixoto, L. Bee, A. Symeonidi, M. S. Schmidt, C. Brenner,  
33 S. Masri, S. A. Benitah, P. Sassone-Corsi., *Cell* **2017**, *170*, 664.  
34  
35 [60] E. M. Gibson, W. P. Williams, 3rd, L. J. Kriegsfeld, *Exp. Gerontol.* **2009**, *44*, 51.  
36  
37 [61] H. Inokawa, Y. Umemura, A. Shimba, E. Kawakami, N. Koike, Y. Tsuchiya, M.  
38 Ohashi, Y. Minami, G. Cui, T. Asahi, R. Ono, Y. Sasawaki, E. Konishi, S. H. Yoo, Z.  
39 Chen, S. Teramukai, K. Ikuta, K. Yagita, *Sci. Rep.* **2020**, *10*, 2569.  
40  
41 [62] E. N. C. Manoogian, S. Panda, *Ageing Res. Rev.* **2017**, *39*, 59.  
42  
43 [63] C. R. Cederroth, U. Albrecht, J. Bass, S. A. Brown, J. Dyhrfeld-Johnsen, F. Gachon,  
44 C. B. Green, M. H. Hastings, C. Helfrich-Forster, J. B. Hogenesch, F. Levi, A. Loudon,  
45 G. B. Lundkvist, J. H. Meijer, M. Rosbash, J. S. Takahashi, M. Young, B. Canlon, *Cell*  
46 *Metab.* **2019**, *30*, 238.  
47  
48 [64] Z. Chen, S. H. Yoo, J. S. Takahashi, *Annu. Rev. Pharmacol. Toxicol.* **2018**, *58*, 231.

- 1  
2  
3  
4 [65] M. Hatori, C. Vollmers, A. Zarrinpar, L. DiTacchio, E. A. Bushong, S. Gill, M.  
5 Leblanc, A. Chaix, M. Joens, J. A. Fitzpatrick, M. H. Ellisman, S. Panda, *Cell Metab.*  
6 **2012**, *15*, 848.  
7  
8 [66] A. Chaix, E. N. C. Manoogian, G. C. Melkani, S. Panda, *Annu. Rev. Nutr.* **2019**, *39*,  
9 291.  
10  
11 [67] S. Miller, T. Hirota, *J. Mol. Biol.* **2020**, *432*, 3498.  
12  
13  
14  
15  
16  
17  
18  
19  
20  
21  
22  
23  
24  
25  
26  
27  
28  
29  
30  
31  
32  
33  
34  
35  
36  
37  
38  
39  
40  
41  
42  
43  
44  
45  
46  
47  
48  
49  
50  
51  
52  
53  
54  
55  
56  
57  
58  
59  
60

For Peer Review

## Figure legends

**Figure 1. Sudachitin is a clock-modulating compound.** (A) Left: Dose-dependent effects of Sudachitin on reporter rhythms in *Bmal1-luc* U2OS cells. Right: quantification of amplitude or period response to Sudachitin doses. Box plot shows the median (bar), values to the 1.5 interquartile ranges (whiskers), and the 25 to 75 percentile range (box). (B) mRNA levels of *Bmal1*, *Per2*, *Rev-erba*, and *Cry1* in U2OS cells by RT-qPCR. (C) Representative images of immunoblot analysis for BMAL1, PER2, REV-ERB $\alpha$ , and CRY1 in U2OS cells. Densitometric analysis of protein levels by immunoblot analysis (lower panels). Values are shown as means  $\pm$  SE ( $n = 3-4$ ,  $n =$  number of independent replicates). # indicates  $p < 0.05$  vs. vehicle.

**Figure 2. Concentrations of Sudachitin were elevated in mouse plasma and tissues after oral administration.** (A) Purity of the Sudachitin compound for oral administration to mice by LC-TOFMS. (B) Concentration of total Sudachitin in mice plasma and tissues at 1 h after oral administration of 100 mg/g body weight (BW) purified Sudachitin compound. (C) Pharmacokinetic study of oral administration of 100 mg/g BW Sudachitin. Sudachitin glucuronide was not detected in adipose tissues, skeletal muscle, and brain. The half-life period ( $t_{1/2}$ ) of Sudachitin and the derivatives are indicated in the graph. Values are shown as means  $\pm$  SE ( $n = 4-5$ ). WAT, white adipose tissue; BAT, Brown adipose tissue; SM, skeletal muscle.

1  
2  
3  
4  
5  
6  
7  
8 **Figure 3. Sudachitin modulates circadian rhythms, sleep/wake cycle, and respiratory**  
9 **exchange (RER) ratio in high-fat diet (HFD)-fed mice. (A)** Representative circadian wheel-  
10 **running actograms illustrating the effect of vehicle (control) or Sudachitin on circadian**  
11 **activities in HFD-fed WT mice. (B)** Left: average wave plots summarizing wheel running  
12 **activity under LD (12 hr light, 12 hr dark, upper panels) or DD (constant darkness, bottom**  
13 **panels) for the indicated groups. Right: daily wheel-running activity during LD or DD**  
14 **conditions for the indicated groups (n = 9-10). (C)** Daily wheel-running period during LD or  
15 **DD conditions for the indicated groups (n = 9-10). (D)** Left: average wave plots of sleep/wake  
16 **cycle (% sleep) under LD condition. Right: daily % sleep under LD conditions for the**  
17 **indicated groups (n = 11-12). (E)** Left: The diurnal rhythms of oxygen consumption ( $VO_2$ ) in  
18 **the four groups of mice under LD condition. Right: daily resting energy expenditure under LD**  
19 **conditions for the indicated groups (n = 11-12). (F)** Left: average wave plots of RER under LD  
20 **condition. Right: daily RER under LD conditions for the indicated groups. Values are shown**  
21 **as means  $\pm$  SE (n = 11-12 per group). Each box plot shows the median (bar), values to the 1.5**  
22 **interquartile ranges (whiskers), and the 25 to 75 percentile range (box). C, Control; S,**  
23 **Sudachitin.**  
24  
25  
26  
27  
28  
29  
30  
31  
32  
33  
34  
35  
36  
37  
38  
39  
40  
41  
42  
43  
44  
45  
46  
47  
48  
49  
50  
51  
52  
53  
54  
55  
56  
57  
58  
59  
60

1  
2  
3  
4 **Figure 4. Sudachitin modulates plasma lipids, and reduces hepatic lipid accumulation in**  
5  
6  
7 **HFD-fed mice. (A) Plasma triglyceride. (B) Plasma non-esterified fatty acid (NEFA). (C)**  
8  
9  
10  
11 Plasma total cholesterol. **(D) Blood glucose. (E) Plasma insulin. (F) Representative images of**  
12  
13  
14 hematoxylin and eosin staining of paraffin embedded-liver sections of 30-week-old mice.  
15  
16  
17 Scale bar = 0.2 mm. **(G) NAFLD activity scores on liver tissue. (H) Liver triglyceride. (I)**  
18  
19  
20  
21 Plasma alanine aminotransferase (ALT). **(J) mRNA level measurements of key genes between**  
22  
23  
24 the control and Sudachitin groups by RT-qPCR. Blood samples were corrected from 15 h-  
25  
26  
27 fasted (Fasted) or non-fasted (Fed) 20-week-old mice. Values are shown as means  $\pm$  SE (n =  
28  
29  
30 11-12 per group). Cont, Control; Sud, Sudachitin; NAFLD, Non-alcoholic fatty liver disease.  
31  
32  
33  
34  
35  
36  
37  
38

39 **Figure 5. Sudachitin modulates diurnal transcriptome in the liver. (A-C) RNA-sequencing**  
40  
41  
42 analysis of liver in 30-week-old HFD-fed mice (n = 2 per group). **(A) Heatmap showing**  
43  
44 differential expression genes between ZT6 and ZT18 ( $p < 0.05$ , fold change  $> 1.5$ ) in each  
45  
46  
47 group. **(B) Venn diagram showing the relationship of transcriptome changes between ZT6 and**  
48  
49 ZT18 in control and Sudachitin group. **(C) Gene ontology (GO) analysis of up-and down-**  
50  
51 regulated transcripts between control and Sudachitin group. **(D) mRNA levels of the**  
52  
53 differential genes between control and Sudachitin group by RT-qPCR. Values are shown as  
54  
55  
56  
57  
58  
59  
60

1  
2  
3  
4 means  $\pm$  SE (n = 5-6 per group). # indicates significant difference ( $p < 0.05$ ) under ANOVA  
5  
6  
7 with Bonferroni's multiple comparison tests. Cont, Control; Sud, Sudachitin; ZT, zeitgeber  
8  
9  
10 time.

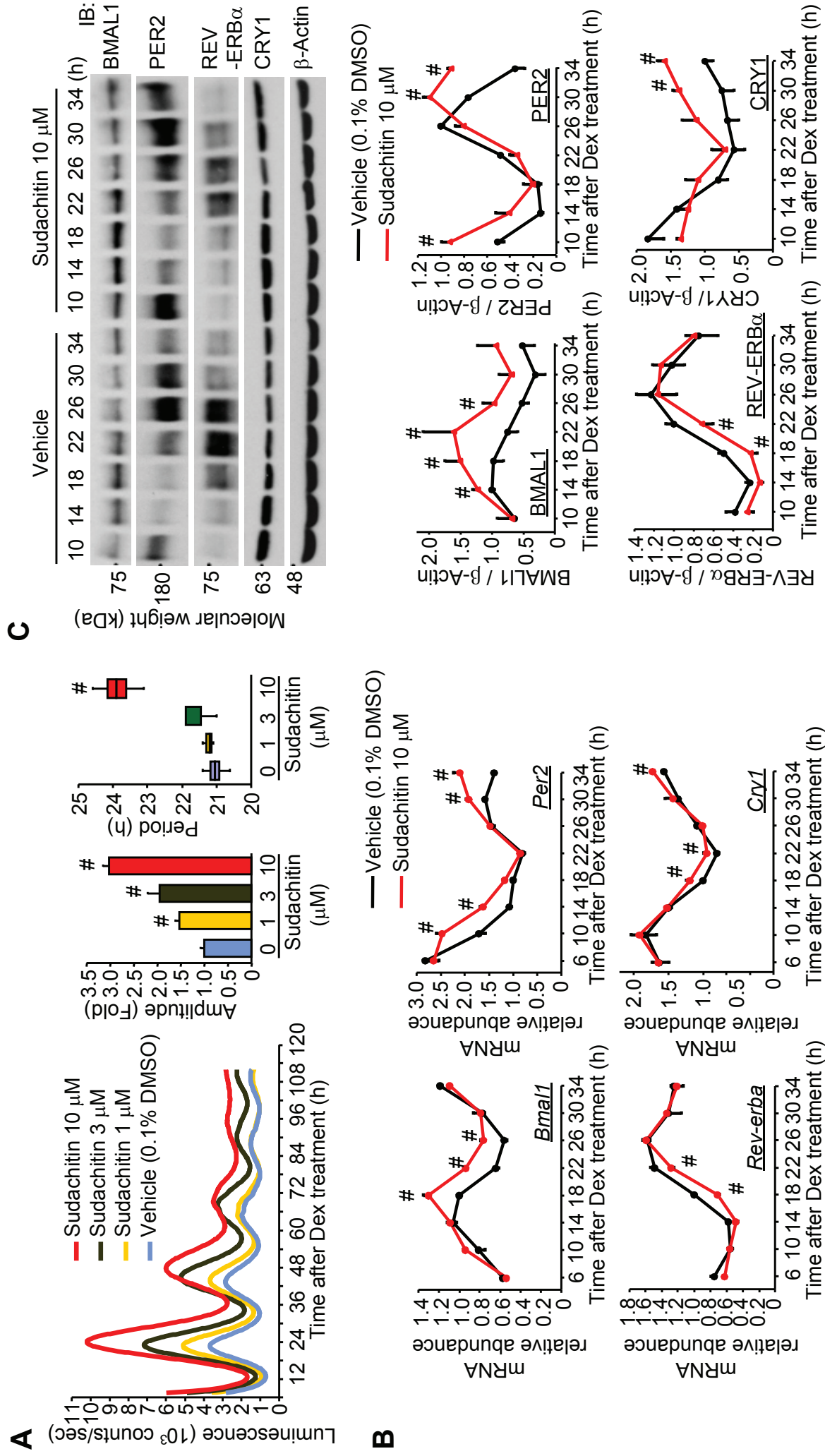
11  
12  
13  
14  
15  
16  
17 **Figure 6. Hydrophilic metabolite profiling in the liver of control or Sudachitin-treated mice.**

18  
19  
20 (A) Heat map showing differential hydrophilic metabolites in the liver between ZT6 and ZT18  
21 ( $p < 0.05$ ) in each group of 30-week-old mice. (B) Venn diagram showing the relationship of  
22 metabolite changes between ZT6 and ZT18 in the control and Sudachitin groups. (C) Principal  
23 component analysis score plot of metabolite profiles in the control and Sudachitin groups. (D)  
24 Enrichment analysis of KEGG pathways of distinct hydrophilic metabolites between ZT6 and  
25 ZT18 in the control and Sudachitin groups. (E-G) The concentrations of metabolites  
26 associated with the citrate cycle (E), branched-chain amino acid metabolism (F), and aromatic  
27 amino acid metabolism (G). The hydrophilic metabolites were measured by CE-TOFMS, as  
28 described in the Material and Methods section. Values are shown as means  $\pm$  SE (n = 5-6 per  
29 group). # indicates significantly difference ( $p < 0.05$ ) under ANOVA with Bonferroni's  
30 multiple comparison tests. Cont, Control; Sud, Sudachitin; ZT, zeitgeber time.  
31  
32  
33  
34  
35  
36  
37  
38  
39  
40  
41  
42  
43  
44  
45  
46  
47  
48  
49  
50  
51  
52  
53  
54  
55  
56  
57  
58  
59  
60

1  
2  
3  
4 **Figure 7. Lipophilic metabolite profiling in the liver of control and sudachitin-treated mice.**

5  
6  
7 (A) Heatmap showing differential lipophilic metabolites in the liver between ZT6 and ZT18 ( $p$   
8  $< 0.05$ ) in each group of 30-week-old mice. (B) Venn diagram showing the relationship of  
9  
10  
11  $< 0.05$ ) in each group of 30-week-old mice. (B) Venn diagram showing the relationship of  
12  
13  
14 metabolite changes between ZT6 and ZT18 in the control and Sudachitin groups. (C) Principal  
15  
16  
17 component analysis score plot of metabolite profiles of the control and Sudachitin groups. (D)  
18  
19  
20 Categories of differentiate lipophilic metabolites between ZT6 and ZT18 in the control and  
21  
22  
23 Sudachitin groups. (E-G) The levels of peptides (E), glycerophospholipids (F), and  
24  
25  
26 sphingolipids (G) in the liver. The lipophilic metabolites were extracted from liver tissues by  
27  
28  
29 the Bligh and Dyer method and measured by LC-TOFMS. Values are shown as means  $\pm$  SE ( $n$   
30  
31  
32 = 5-6 per group). # indicates significantly difference ( $p < 0.05$ ) under ANOVA with  
33  
34  
35 Bonferroni's multiple comparison tests. Cont, Control; Sud, Sudachitin; ZT, zeitgeber time;  
36  
37  
38 PC, phosphatidylcholine; PI, phosphatidylinositol; Cer, ceramide.  
39  
40  
41  
42  
43  
44  
45  
46  
47  
48  
49  
50  
51  
52  
53  
54  
55  
56  
57  
58  
59  
60

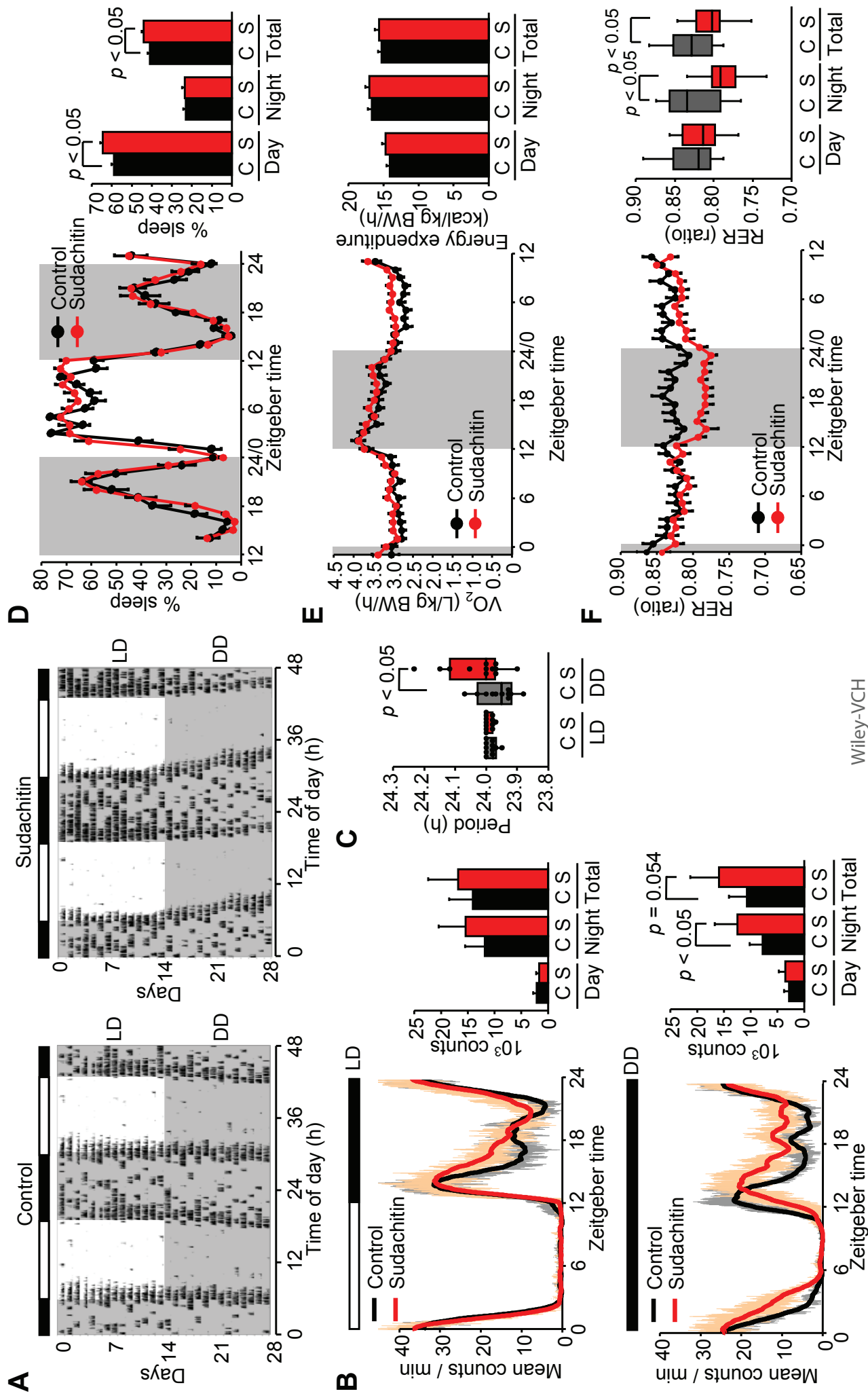
Mawatari K, et al., Fig. 1-R3



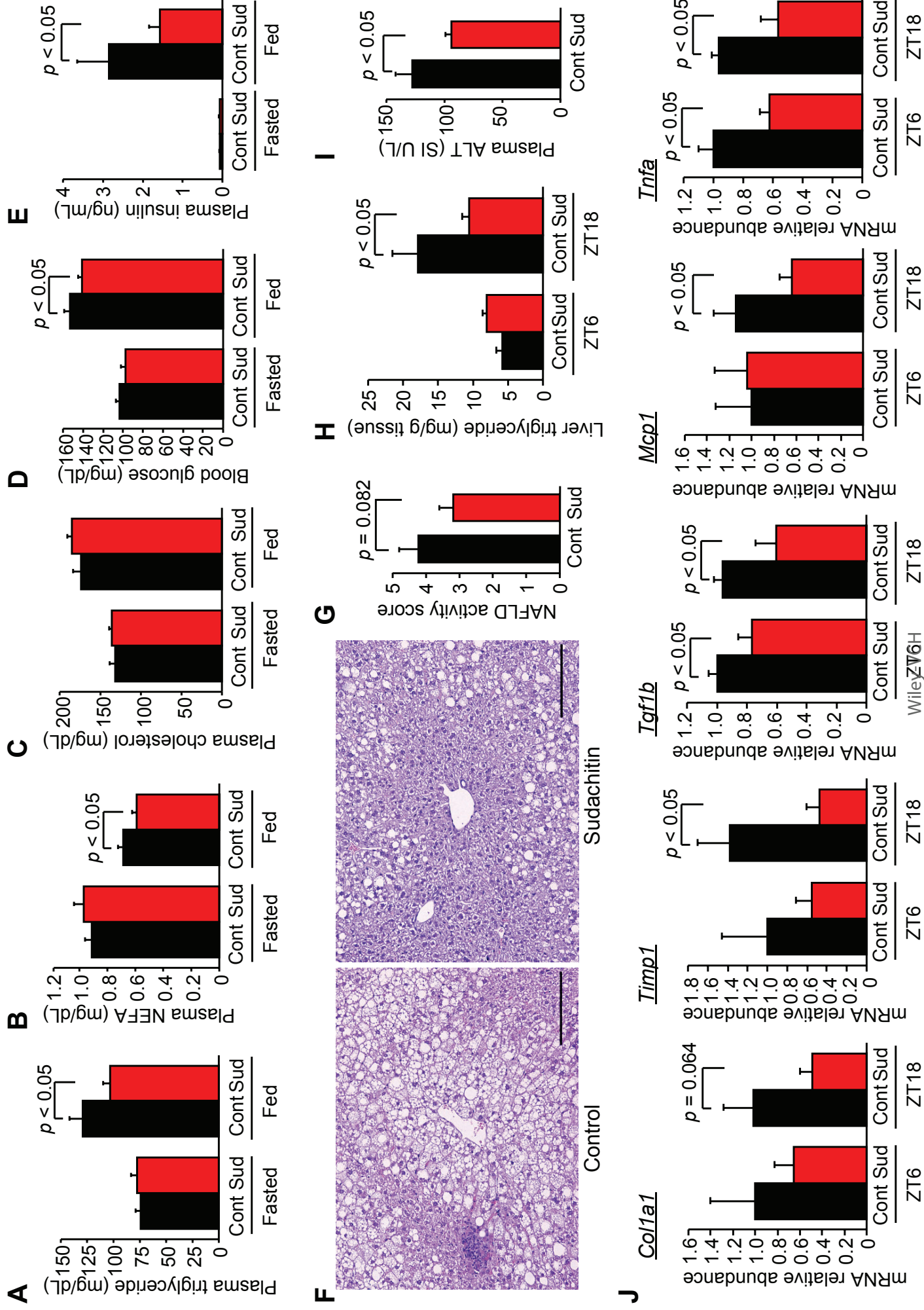
1  
2  
3  
4  
5  
6  
7  
8  
9  
10  
11  
12  
13  
14  
15  
16  
17  
18  
19  
20  
21  
22  
23  
24  
25  
26  
27  
28  
29  
30  
31  
32  
33  
34  
35  
36  
37  
38  
39  
40  
41

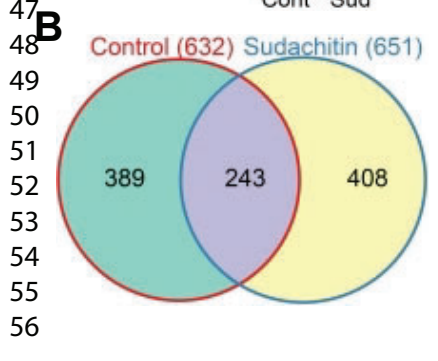
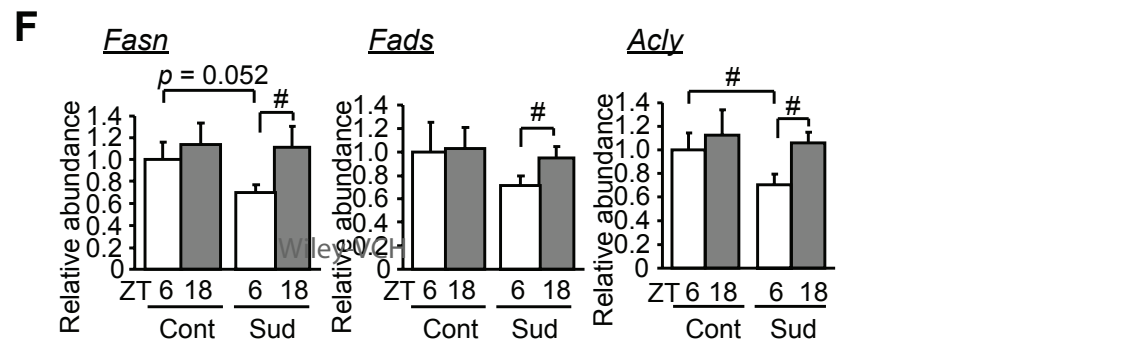
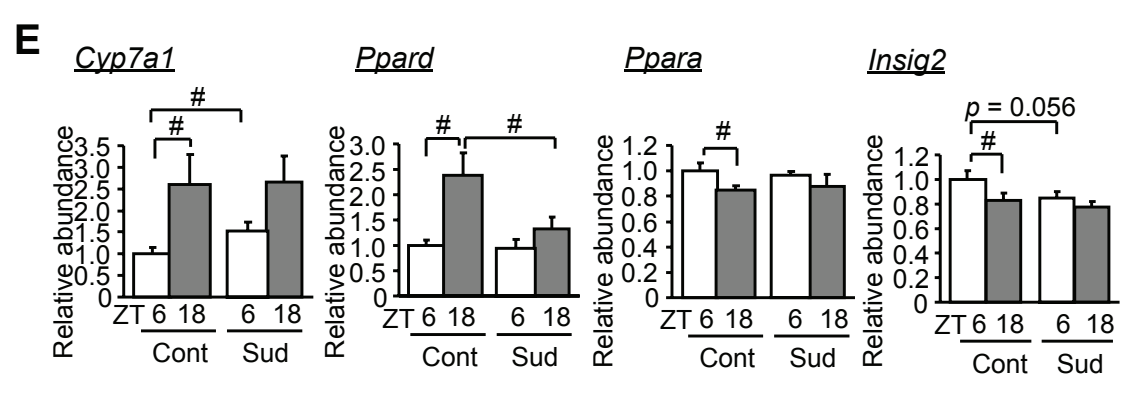
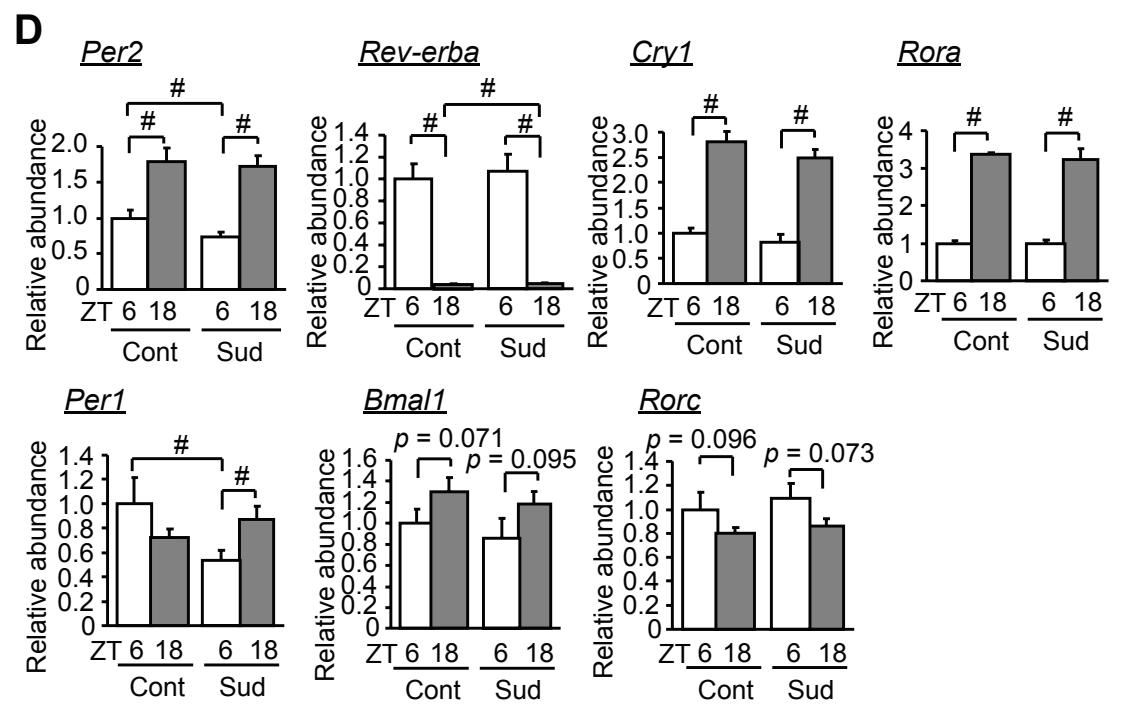
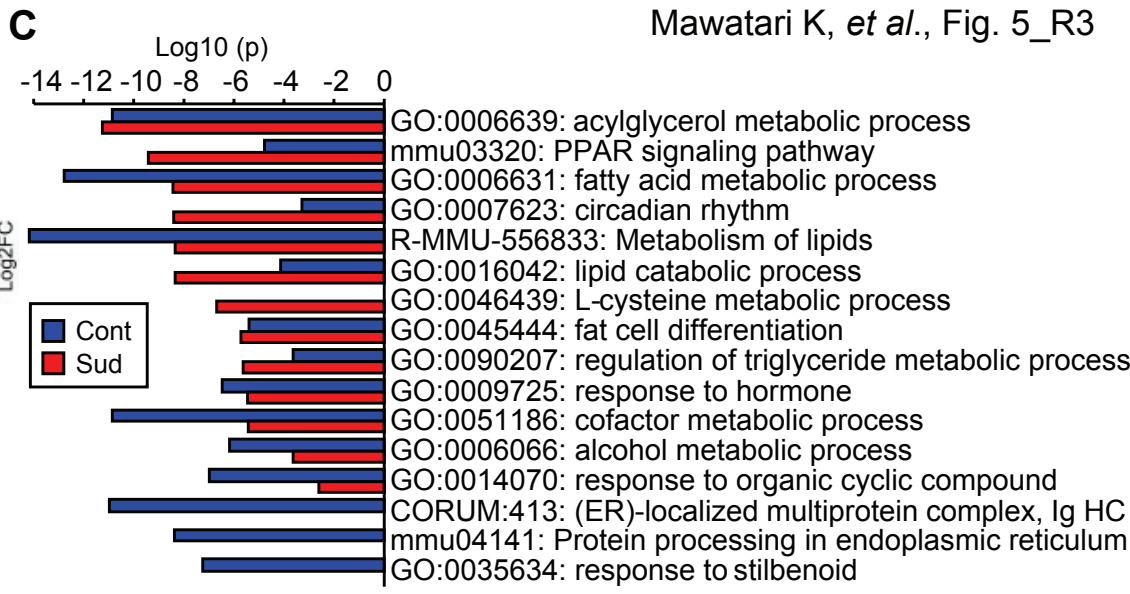
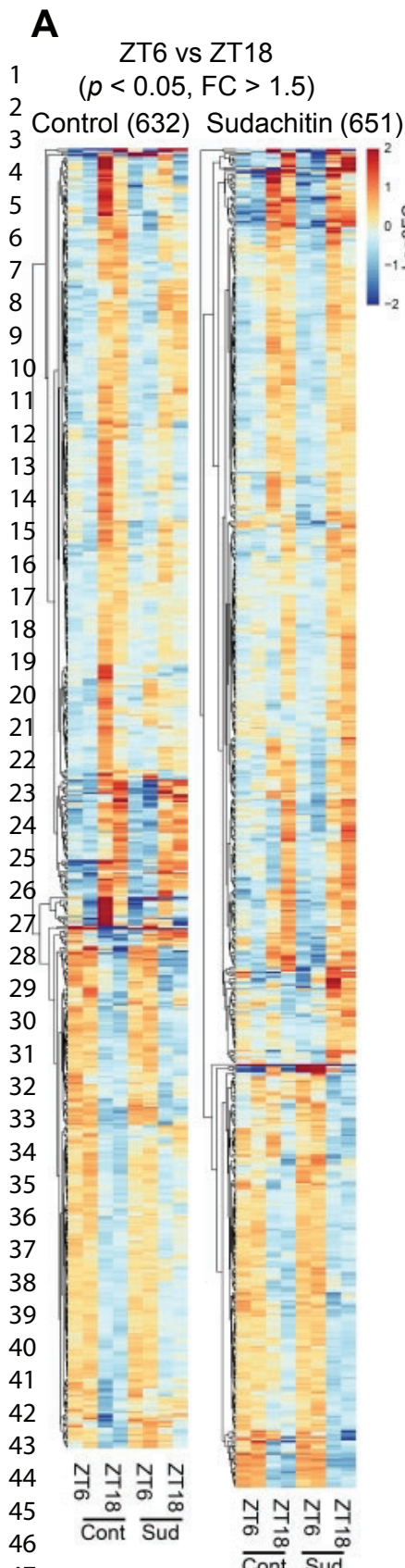


Mawatari K, et al., Fig. 3-R3

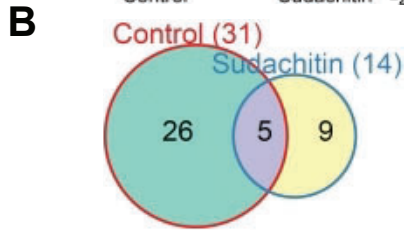
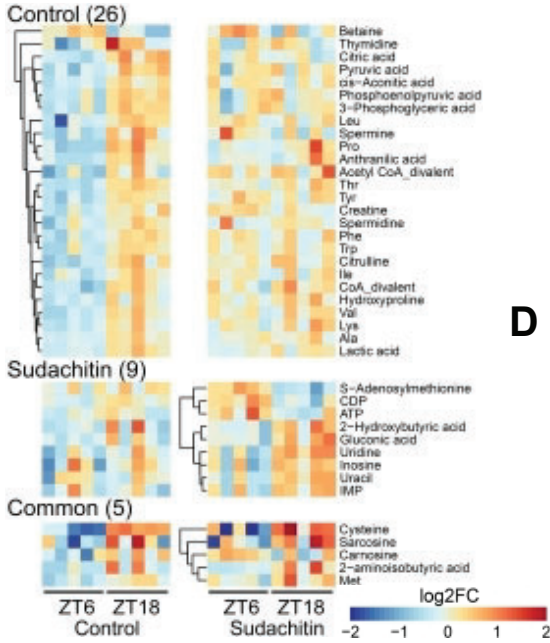


1  
2  
3  
4  
5  
6  
7  
8  
9  
10  
11  
12  
13  
14  
15  
16  
17  
18  
19  
20  
21  
22  
23  
24  
25  
26  
27  
28  
29  
30  
31  
32  
33  
34  
35  
36  
37  
38  
39  
40  
41

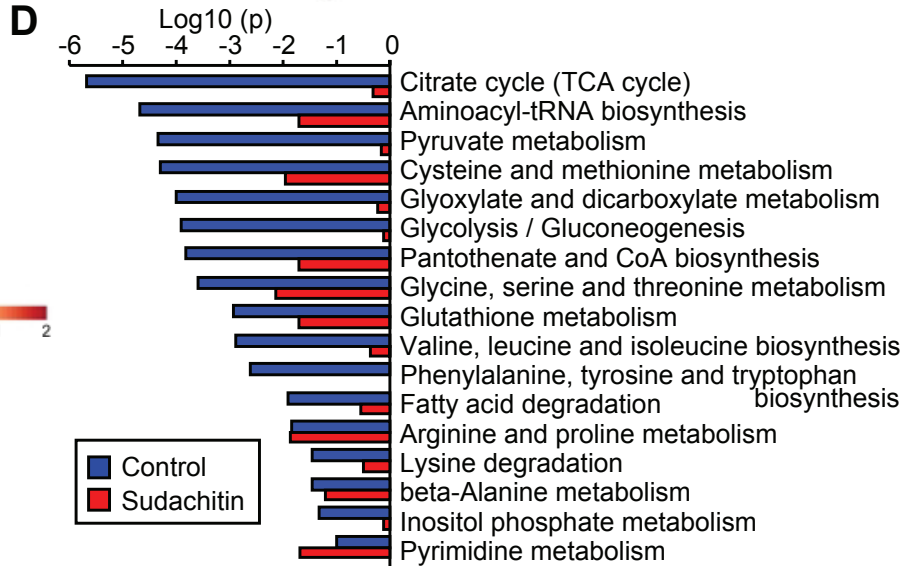
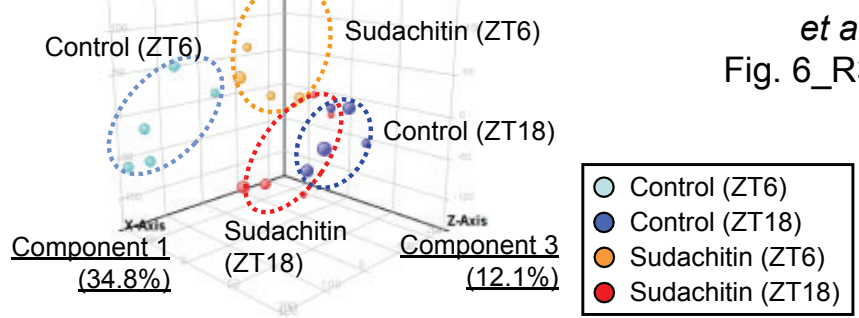




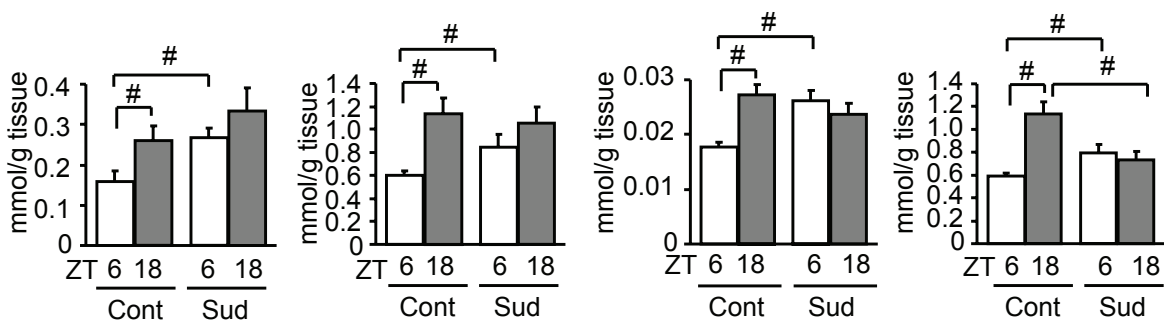
**A** ZT6 vs ZT18 ( $p < 0.05$ )



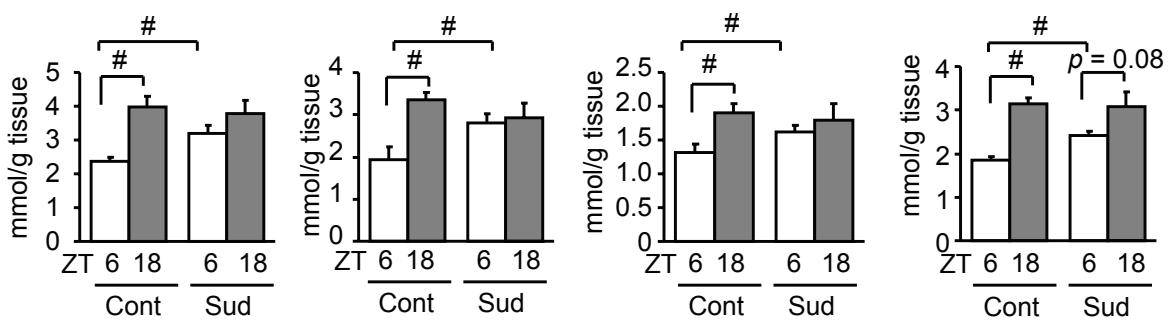
**C** Component 2 (14.4%)



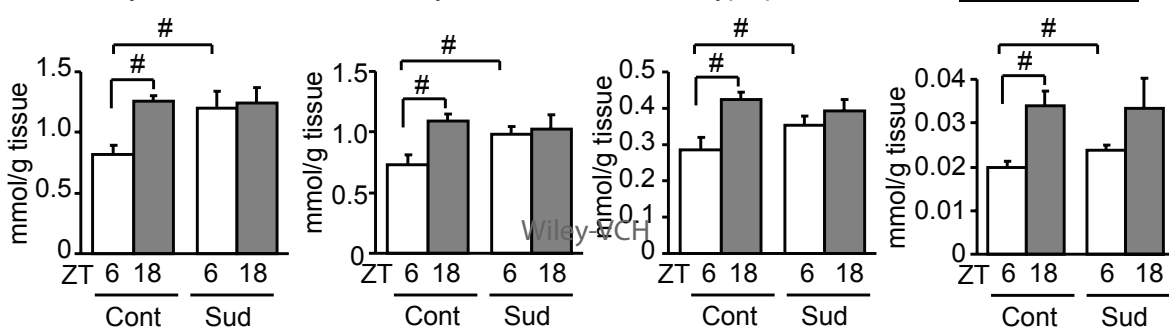
**E** Acetyl-Coenzyme A

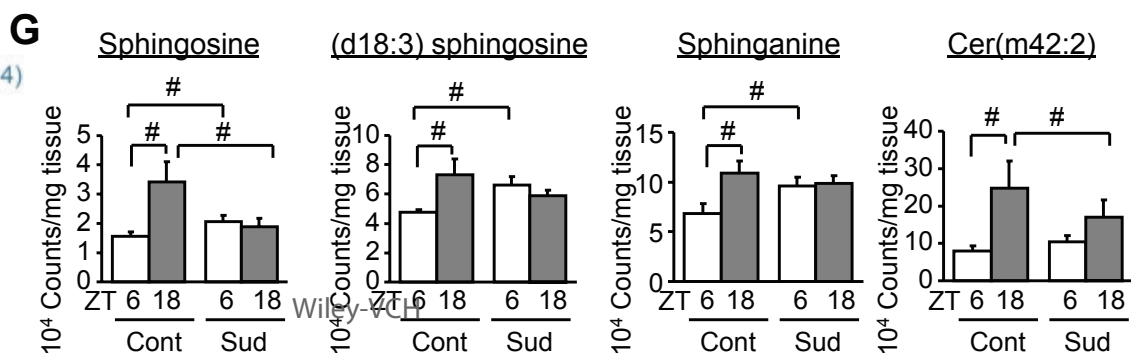
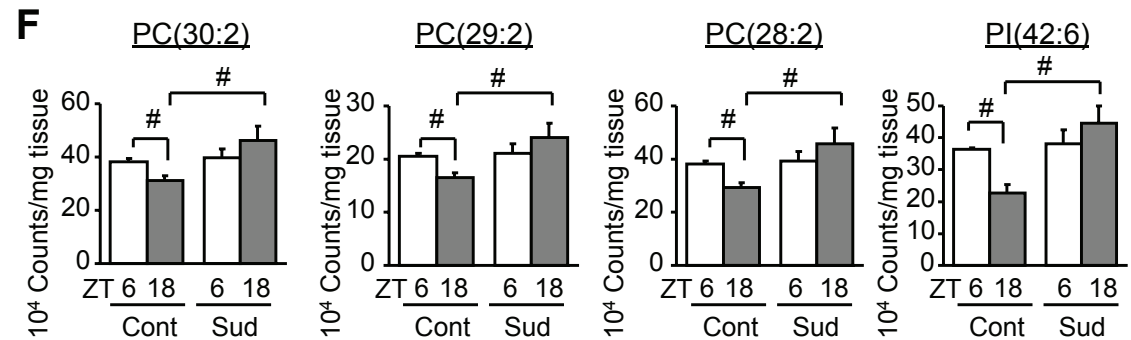
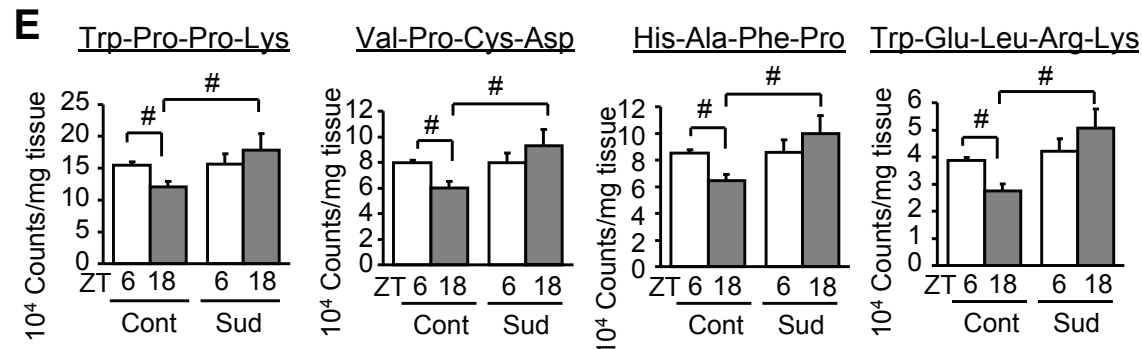
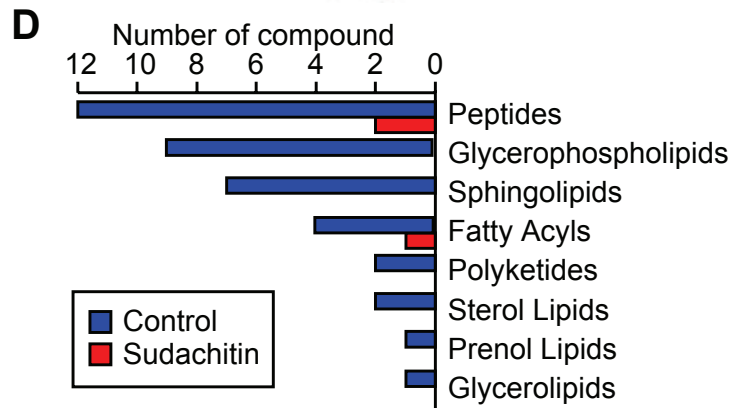
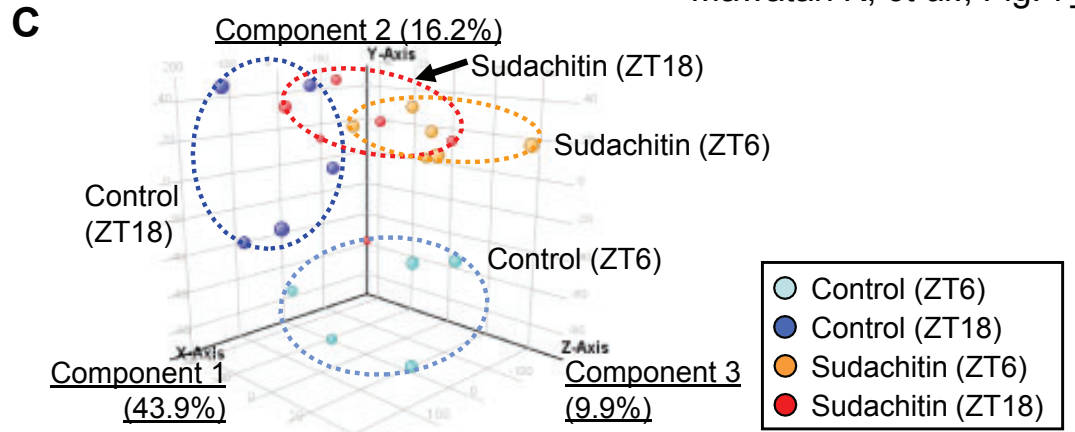
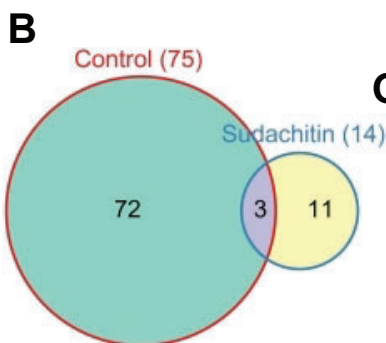
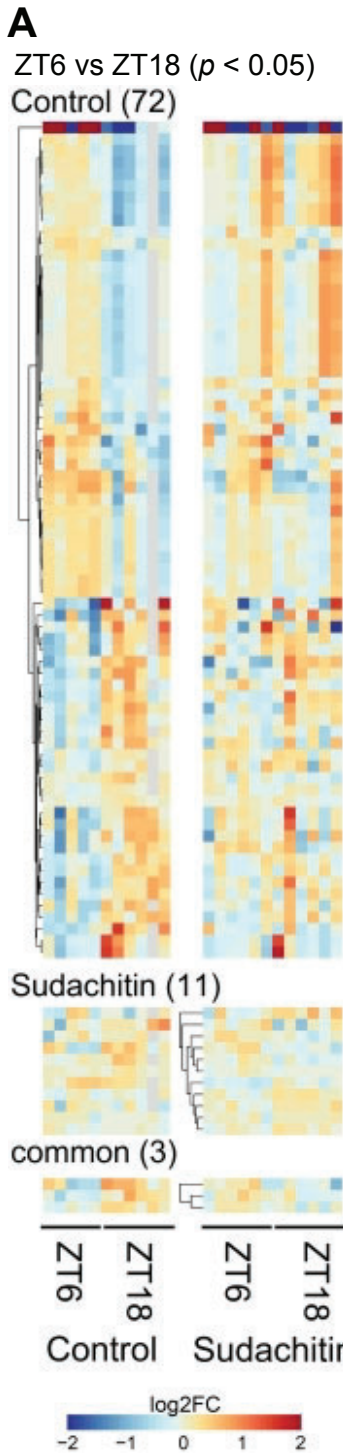


**F** Valine



**G** Tyrosine

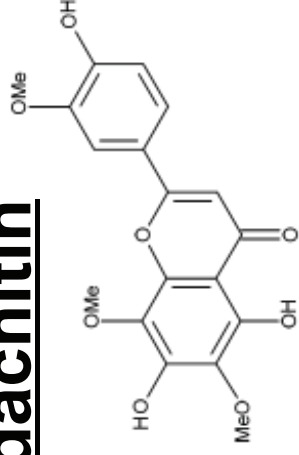




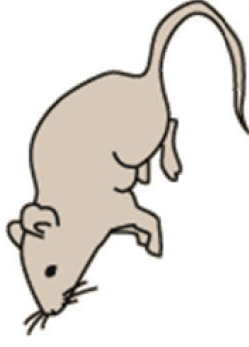
# Sudachitin



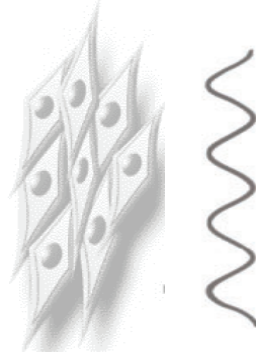
*Citrus sudachi*



High fat diet-fed mice

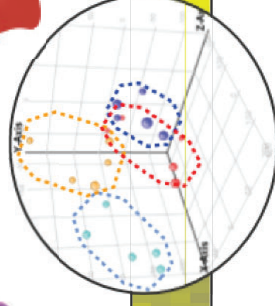
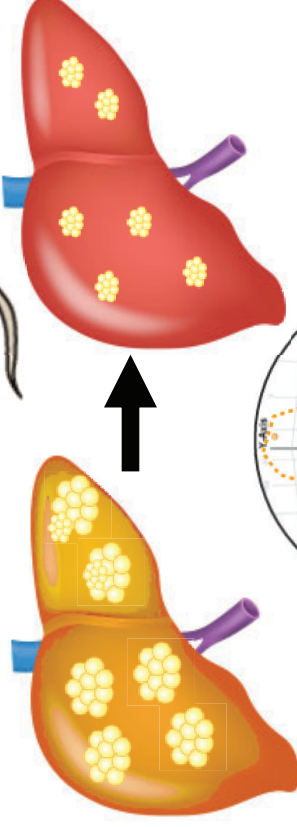


Circadian reporter cells



Modulation of circadian gene expression

Improved liver physiology  
(lipid accumulation,  
fibrosis, inflammation)



Diurnal transcriptomic and metabolomic alteration

- Sudachitin is a polymethoxylated flavone (PMF) enriched in *Citrus sudachi*.
- Sudachitin modulates circadian rhythms *in vitro* and *in vivo*
- Sudachitin improves clock-associated systemic and liver physiology
- Integrative omics revealed altered expression and metabolite landscapes

For Peer Review